Computers

by Yingjie Cui, Xu Li, Zhongxian Chen and Yan Li

Logical OperatorOperator

Search Text

Search Type

add_circle_outline

remove_circle_outline

Journal Description

Computers is an international, scientific, peer-reviewed, open access journal of computer science, including computer and network architecture and computer–human interaction as its main foci, published monthly online by MDPI.

- Open Access— free for readers, with article processing charges (APC) paid by authors or their institutions.
- **High Visibility:** indexed within Scopus, ESCI (Web of Science), dblp, Inspec, Ei Compendex, and other databases.
- **Journal Rank:** JCR - Q2 (Computer Science, Interdisciplinary Applications) / CiteScore - Q1 (Computer Science (miscellaneous))
- **Rapid Publication:** manuscripts are peer-reviewed and a first decision is provided to authors approximately 17.5 days after submission; acceptance to publication is undertaken in 3.9 days (median values for papers published in this journal in the second half of 2025).
- **Recognition of Reviewers:** reviewers who provide timely, thorough peer-review reports receive vouchers entitling them to a discount on the APC of their next publication in any MDPI journal, in appreciation of the work done.
- **Journal Cluster of Artificial Intelligence:** *AI*, *AI in Medicine*, *Algorithms*, *BDCC*, *MAKE*, *MTI*, *Stats*, *Virtual Worlds* and *Computers*.

Impact Factor: 4.2 (2024); 5-Year Impact Factor: 3.5 (2024)

Latest Articles

46 pages, 5023 KB

Open AccessReview

A Survey of Fault and Intrusion Tolerance Approaches for Scientific Workflow Scheduling in Cloud Computing

by **Mazen Farid**, **Oluwatosin Ahmed Amodu**, **Heng Siong Lim**, **Jamil Abedalrahim Jamil Alsayaydeh**, **Mohammed Fadhl Abdullah** and **Faten A. Saif**

Computers **2026**, *15*(5), 304; https://doi.org/10.3390/computers15050304 (registering DOI) - 10 May 2026

Abstract

To provide reliable services in the cloud, fault tolerance is perhaps the most important consideration. The inherent sensitivity to failure hampers cloud services' performance and reliability. As a result, fault tolerance becomes a required characteristic to maintain reliability, which is difficult to provide [...] Read more.

To provide reliable services in the cloud, fault tolerance is perhaps the most important consideration. The inherent sensitivity to failure hampers cloud services' performance and reliability. As a result, fault tolerance becomes a required characteristic to maintain reliability, which is difficult to provide due to the dynamic architecture and complex inter-dependencies. To address the issues of cloud reliability, many fault-tolerant approaches have been developed in the literature. This paper presents a recent research survey that seeks to classify the various faults and intrusion tolerance architectures. Furthermore, it provides a thorough critical analysis of existing fault and intrusion tolerance, as well as combined approaches, aimed at enhancing the dependability, availability, and execution of cloud services. The report also includes a comparison of the studied systems' framework based on various essential criteria such as cost, makespan, reliability, security, resource utilization, energy consumption, and failure ratio. This study aims to comprehensively review this subject for researchers to draw insights from existing patterns in the literature and provide deeper perspectives into some of the challenging issues and prospects. This will enhance the development of highly resilient fault-tolerant and intrusion-resistive scheduling algorithms for current and future cloud applications. Full article

► Show Figures

17 pages, 7767 KB

Open AccessArticle

EEG Fatigue Judgment Method Based on Approximate Nearest Neighbor Search

Computers **2026**, *15*(5), 303; https://doi.org/10.3390/computers15050303 (registering DOI) - 10 May 2026

Abstract

Fatigue seriously affects work efficiency and brings potential safety hazards, and electroencephalogram (EEG) serves as a valuable physiological indicator for fatigue monitoring, as it directly reflects underlying brain neural activity. A key characteristic in EEG fatigue research is that the feature spaces of [...] Read more.

Fatigue seriously affects work efficiency and brings potential safety hazards, and electroencephalogram (EEG) serves as a valuable physiological indicator for fatigue monitoring, as it directly reflects underlying brain neural activity. A key characteristic in EEG fatigue research is that the feature spaces of pre-fatigue and post-fatigue EEG signals exhibit obvious spatial separation—this separation is caused by significant changes in brain electrical activity when the human body transitions from a normal awake state to a fatigue state. Existing EEG-based fatigue judgment methods mostly focus on binary classification, which fails to fully leverage the inherent spatial separation characteristic of pre-fatigue and post-fatigue feature spaces, making it difficult to achieve simple, efficient, and accurate fatigue judgment. To address this problem, this paper proposes an EEG fatigue judgment method based on feature space spatial separation and Approximate Nearest Neighbor Search (ANNS). The 16-channel pre-fatigue (Group A) and post-fatigue (Group B) EEG signals acquired from seven subjects are segmented and subjected to feature extraction, projecting the signals into a unified feature space. An ANNS index is constructed using feature vectors from both Group A and Group B, with each vector annotated by its corresponding class label. A separate test set (Group C) is utilized, and the k-nearest neighbors of each test feature vector are retrieved from the built ANNS index. The mental fatigue state is then identified via majority voting according to the class

labels of the k-nearest neighbors. Experimental results demonstrate that the proposed method can effectively exploit the spatial separation between pre-fatigue and post-fatigue feature distributions, yielding an average single-subject classification accuracy of approximately 90%. Full article

► Show Figures

22 pages, 2892 KB

Open AccessArticle

An Efficient Quantum-Dot Cellular Automata Memory Architecture for Internet of Things Systems

by **B. S. Premananda**, **Mohsen Vahabi**, **Muhammad Zohaib**, **Seyed-Sajad Ahmadpour**, **M. Barath** and **K. R. Sreesha**

Computers **2026**, *15*(5), 302; https://doi.org/10.3390/computers15050302 (registering DOI) - 9 May 2026

Abstract

Internet of Things (IoT) nodes continuously acquire, buffer, and transmit sensor data under strict constraints on area, latency, and energy consumption. However, conventional complementary metal–oxide–semiconductor (CMOS)-based memory-access circuits face increasing power loss, parasitic effects, interconnect complexity, and sensitivity to process variations at the [...] Read more.

Internet of Things (IoT) nodes continuously acquire, buffer, and transmit sensor data under strict constraints on area, latency, and energy consumption. However, conventional complementary metal–oxide–semiconductor (CMOS)-based memory-access circuits face increasing power loss, parasitic effects, interconnect complexity, and sensitivity to process variations at the nanoscale. To address these limitations, this paper proposes a quantum-dot cellular automata (QCA)-based decoder-driven static random-access memory (SRAM)-access architecture for compact and energy-efficient IoT perception-layer memory. The proposed framework integrates three main components: a majority-logic RAM cell with feedback-based storage and non-destructive readout, a compact 2 × 4 decoder with enable and auxiliary asynchronous set/reset control, and a 1 × 4 SRAM array in which the decoder is embedded to reduce routing and clocking overhead. The circuit layouts were implemented and functionally verified using QCADesigner 2.0.3, while the energy behavior was evaluated using QCADesigner-E. Simulation results confirm correct write/read (W/R) and address-selection behavior. The proposed 2 × 4 decoder achieves 86 QCA cells, 0.08 μm^2 occupied area, and one clocking unit, reducing cell count, area, and clocking by 48.19%, 50.00%, and 20.00%, respectively, compared with the best selected decoder baseline. The integrated 1 × 4 SRAM array achieves 684 cells and 14 clocking units, improving timing by 30.00% compared with the closest SRAM-array baseline. These results demonstrate that the proposed QCA-based memory-access structure provides a compact and low-overhead solution for energy-constrained IoT communication systems. Full article

15 pages, 664 KB

Open AccessArticle

Quantifying the Impact of Signal Simplification, Data Quantity, and Task Difficulty on Vision Transformer Performance for ECG Rhythm Classification

by **Jarod P. Hartley** and **W. Joseph MacInnes**

Computers **2026**, *15*(5), 301; https://doi.org/10.3390/computers15050301 (registering DOI) - 9 May 2026

Abstract

Vision transformers (ViTs) have demonstrated considerable promise for classifying electrocardiogram (ECG) rhythms. However, much of the existing research is conducted in highly controlled, data-sterile settings that fail to reflect the substantial variability present in real-world ECG signals. This paper seeks to address this [...] Read more.

Vision transformers (ViTs) have demonstrated considerable promise for classifying electrocardiogram (ECG) rhythms. However, much of the existing research is conducted in highly controlled, data-sterile settings that fail to reflect the substantial variability present in real-world ECG signals. This paper seeks to address this gap by examining how signal simplification, data quantity, and task difficulty influence the performance of the SwinV2 ViT model in ECG rhythm classification. Through systematic analysis, we highlight that classifying highly abstracted signals yields only a limited impact on model performance, with all models achieving over 95% accuracy, while the amount of training data plays a crucial role with an almost 15% accuracy difference between the models trained on the most data and the least data. Finally, our analysis shows the model's ability to effectively adapt to an increased class count, which is essential due to the varying nature of ECG diagnosis. In summary, these results highlight the importance of carefully balancing data clarity, dataset size, and diagnostic variety when designing ECG classification systems. Achieving this balance is crucial for building reliable and scalable AI solutions for cardiac assessment. Full article

17 pages, 1989 KB

Open AccessArticle

An Integrated Open-Source Software System for the Generation and Analysis of Subject-Specific Blood Flow Simulation Ensembles

by **Simon Leistikow**, **Thomas Miro**, **Adrian Kummerländer**, **Ali Nahardani**, **Katja Grün**, **Marcus Franz**, **Verena Hoerr**, **Mathias J. Krause** and **Lars Linsen**

Computers **2026**, *15*(5), 300; https://doi.org/10.3390/computers15050300 (registering DOI) - 9 May 2026

Abstract

Hemodynamic analysis of blood flow is critical for diagnosing cardiovascular diseases and investigating cardiovascular parameters, such as aneurysms and wall shear stress. For subject-specific analyses, the anatomy and blood flow of the subject can be captured non-invasively using structural and 4D Magnetic Resonance [...] Read more.

Hemodynamic analysis of blood flow is critical for diagnosing cardiovascular diseases and investigating cardiovascular parameters, such as aneurysms and wall shear stress. For subject-specific analyses, the anatomy and blood flow of the subject can be captured non-invasively using structural and 4D Magnetic Resonance Imaging (MRI), respectively. Computational fluid dynamics (CFD), on the other hand, can be used to generate blood flow simulations. To generate and analyze subject-specific blood flow simulations, MRI and CFD have to be brought together. We present an interactive, customizable, and user-oriented visual analysis tool that integrates measured data and CFD simulations. Thus, our open-source tool supports both medical and numerical analysis workflows. It enables the creation of simulation ensembles with a high variety of parameters. Furthermore, it allows for visual and analytical examination of simulations and measurements through 2D embeddings. To demonstrate the effectiveness of our tool, we applied it to three real-world use cases, showcasing its ability to configure simulation ensembles and analyze blood flow. We evaluated our example cases together with

MRI and CFD experts. By combining the strengths of both CFD and MRI, our tool provides a comprehensive understanding of hemodynamic parameters, facilitating accurate analysis of hemodynamic biomarkers. Full article

29 pages, 3102 KB

Open AccessArticle

ASL Recognition and Game-Based Interaction: A Machine Learning—Driven, Gamified and Accessible Vocabulary Learning System for Deaf Learners

by **Stefanie Amiruzzaman**, **Raga Mouni Batchu**, **Md Amiruzzaman**, **Linh Ngo** and **M. Ali Akber Dewan**

Abstract

Digital learning tools for American Sign Language (ASL) often lack the interactive depth necessary to engage learners effectively. This paper introduces a novel, browser-based word search game designed to facilitate ASL vocabulary familiarization through gamified interaction. The system employs a two-tier architecture consisting [...] Read more.

Digital learning tools for American Sign Language (ASL) often lack the interactive depth necessary to engage learners effectively. This paper introduces a novel, browser-based word search game designed to facilitate ASL vocabulary familiarization through gamified interaction. The system employs a two-tier architecture consisting of a React-based frontend and a Flask-based backend. At its core, the application integrates a lightweight, skeleton-based Isolated Sign Language Recognition (ISLR) model, utilizing a Stacked Transformer-based Spatial-Temporal Attention Network to enable real-time webcam-based word entry during the configuration phase. This model, trained on the WLASL-100 dataset, achieves a Top-5 test accuracy of 88.48% with an average model inference latency of 141 ms, enabling real-time webcam input without proprietary hardware. Furthermore, we implement a constraint-satisfaction puzzle generation algorithm that achieves a 100% success rate in creating interlocked, multi-directional grids. Our results demonstrate that merging computer vision with pedagogical game mechanics provides an accessible, high-performance tool for the Deaf and Hard-of-Hearing (DHH) community, bridging the gap between static instruction and active linguistic practice. Full article

► Show Figures

26 pages, 2542 KB

Open AccessArticle

A Multi-Source Pipeline for Extracting Traditional-Style Chinese Melody Data from Symbolic Files and Score Images

by **Xuanfei Zhou**, **Yinxuan Huang**, **Sining Han** and **Jiangyao Bai**

Abstract

Large-scale symbolic melody datasets are essential for data-driven music information retrieval and generation, yet traditional-style Chinese melodies remain scattered across heterogeneous score formats and image sources. Existing extraction pipelines typically focus on single modalities—either MIDI archives or standard staff notation—and lack unified handling [...] Read more.

Large-scale symbolic melody datasets are essential for data-driven music information retrieval and generation, yet traditional-style Chinese melodies remain scattered across heterogeneous score formats and image sources. Existing extraction pipelines typically focus on single modalities—either MIDI archives or standard staff notation—and lack unified handling for numbered musical notation (Jianpu) and automated quality assurance. We propose the Multi-Source Melody Pipeline (MSMP), a *systems-integration prototype* whose front-end admits MIDI, MusicXML, Jianpu images, and staff images, and whose back-end converges on a standardized event-level representation; the present case study exercises the image branch—in particular the Jianpu branch, through a Gemini-2.5-flash vision language model—and treats the MIDI/MusicXML ingestion paths as architectural slots that are wired in but not experimentally validated in this submission. The system employs notation-aware routing to direct score images to appropriate backends (a VLM for Jianpu and rule-based OMR for staff) and enforces a *structural* validity gate (schema conformance plus at least one melodic track with at least one musical event) on every candidate segment. Validation on a 292-page representative prototype cohort yielded an 80.1% *structural-acceptance* rate—explicitly not a transcription accuracy number—and a newly added ground-truth benchmark on 50 manually annotated Jianpu pages reports 95.8% time-signature exact accuracy, 77.1% tonal-pitch-class key accuracy, 100% tempo agreement within

±5

BPM, and, on a 10-page note-level subset, a mean first-16-note pitch F1 of 0.898 (octave-sensitive) with a Symbol Error Rate of 0.150. A companion 10-page $K = 3$ self-consistency audit indicates that metadata errors are systematic rather than stochastic. This work, therefore, contributes a reproducible integration *architecture* and a quantitative baseline on the Jianpu branch, rather than a new OMR algorithm, a new dataset release, or a fully benchmarked multi-format corpus; ongoing work addresses out-of-distribution classifier evaluation, comparison against dedicated Jianpu OMR baselines, and release of a copyright-cleared corpus. Full article

► Show Figures

21 pages, 2357 KB

Open AccessArticle

Integrating Thesaurus-Based Knowledge into Transformer Models for Semantic Understanding of Domain-Specific Texts

by **Bayangali Abdygalym**, **Saule Tazhibayeva**, **Madina Sambetbayeva**, **Aigerim Yerimbetova**, **Roman Taberkhan**, **Manzura Abjalova**, **Aidos Sabdenov** and **Elmira Daiyrbayeva**

Abstract

Integrating structured linguistic resources into deep learning architectures represents a key challenge in domain-oriented NLP. This study proposes a framework for incorporating knowledge from a military thesaurus of the Ground Forces, structured according to the XML Zthes standard, into pre-trained transformed language models, [...] Read more.

Integrating structured linguistic resources into deep learning architectures represents a key challenge in domain-oriented NLP. This study proposes a framework for incorporating knowledge from a military thesaurus of the Ground Forces, structured according to the XML Zthes standard, into pre-trained transformed language models, including KazBERT, multilingual BERT, and XLM-RoBERTA. The approach addresses two interrelated tasks in specialized terminology processing: concept linking and semantic search. Unlike existing knowledge-injection methods designed primarily for general-domain applications, this framework formalizes the mapping of Zthes elements, such as Term, Broader term, Narrower term, Related term, ScopeNote, Language, and Source into structured textual representations that can be directly processed by transformer architectures. Fine-tuning is conducted on a dataset of 18,400 training instances automatically generated from the thesaurus, including synonym pairs, hierarchical relations (hyperonymy and hyponymy), associative links, and

definitional descriptions. Experimental evaluation demonstrated that thesaurus-enriched models outperform baseline architectures across all major metrics. XLM-RoBERTA model achieves F1 = 0.84 and Top-5 accuracy = 0.94 in the concept linking task, representing a five-point improvement over the baseline. The model reaches Macro-F1 = 0.84 across four relation types. Results obtained on a specialized test set derived from terminology databases of Kazakhstan's Armed Forces confirm robust cross-lingual generalization across Kazakh, Russian and English military discourse. Full article

► Show Figures

31 pages, 1116 KB

Open AccessArticle

AI-Driven Clustering-Based Stratification of Allergic Patients Towards Smart Healthcare Systems in Southern Italy

by **Stefano Palazzo**, **Esra Hazar**, **Arife Uslu Gokceoglu**, **Giovanni Zambetta**, **Roberto Caldelli** and **Claudio Loconsole**

Abstract

A clustering analysis was conducted to identify distinct patient subgroups with White Blood Cells (WBC) count alongside Age and Total Immunoglobulin E (IgE) biomarkers. All data were obtained from a coordinated primary care network operating in Apulia (Southern Italy). We analyzed 300 patient [...] Read more.

A clustering analysis was conducted to identify distinct patient subgroups with White Blood Cells (WBC) count alongside Age and Total Immunoglobulin E (IgE) biomarkers. All data were obtained from a coordinated primary care network operating in Apulia (Southern Italy). We analyzed 300 patient records, performed preprocessing and exploratory data analysis, and then applied unsupervised clustering directly to the standardized three-variable feature space (Age, WBC, and Total IgE), followed by supervised validation steps. Several algorithms were applied for clustering. Among the evaluated methods, K-means and Spectral Clustering showed the most favorable internal validation profiles, based on Silhouette Score (SS), Calinski–Harabasz Index (CH), and Davies–Bouldin Index (DB). K-means achieved the best scores (SS = 0.406, CH = 190.00, DB = 0.900), closely followed by Spectral Clustering (SS = 0.398, CH = 182.57, DB = 0.936), outperforming Agglomerative Clustering (SS = 0.361, CH = 160.41, DB = 1.016) and Gaussian Mixture Models (SS = 0.233, CH = 103.89, DB = 1.289). Post-clustering ANOVA analyses indicated significant differences in WBC, age, and total IgE across the five consensus clusters. An evaluation of cluster internal separability occurred through the training of a Random Forest classifier to predict cluster membership. The results indicate internal cluster separability within the analyzed dataset, but more external verification and clinical evidence are necessary for validation. The research group established clinical descriptions along with suggested treatment plans and detected co-existing diseases to help validate model-based findings. A simplified cluster-informed clinical summary based on biomarker ranges was derived to support interpretation of the identified patient profiles. This integrated method preliminarily suggests that patient strata may be identified from routine clinical variables, while highlighting the importance of internal validation and clinical interpretability in clustering research. Full article

► Show Figures

23 pages, 1945 KB

Open AccessArticle

A Self-Adaptive LLM-Based Framework for Automated Extraction and Structuring of Earthquake Information from Heterogeneous Web Sources

by **Assem Turarbek**, **Diana Rakhimova**, **Yeldos Adetbekov** and **Azat Nurgali**

Abstract

The rapid growth of heterogeneous web sources has created significant challenges for the automated extraction and structuring of critical domain-specific information, particularly in real-time seismic monitoring scenarios. Despite the existence of official governmental reporting systems, relevant earthquake-related data are often distributed across diverse [...] Read more.

The rapid growth of heterogeneous web sources has created significant challenges for the automated extraction and structuring of critical domain-specific information, particularly in real-time seismic monitoring scenarios. Despite the existence of official governmental reporting systems, relevant earthquake-related data are often distributed across diverse online platforms with highly variable and dynamically evolving HTML (HyperText Markup Language) structures, leading to incomplete, delayed, or inconsistent information retrieval. Existing rule-based and semi-automated approaches lack scalability and robustness under such conditions. To address this gap, this study proposes a self-adaptive framework based on large language models (LLMs) for the automated extraction and structuring of earthquake-related web content. The proposed approach integrates transformer-based schema generation, repository-guided schema matching, and an iterative refinement mechanism, enabling the system to dynamically adapt to heterogeneous document structures. A formal utility-based decision mechanism is introduced to optimize schema selection and reuse, while embedding-based similarity modeling facilitates efficient transfer of extraction patterns across structurally related webpages. The experimental evaluation was conducted on a heterogeneous benchmark dataset comprising multiple web domains with diverse structural characteristics. The results demonstrate that the proposed framework achieves a success rate of 85% across all evaluated models, with the best-performing configuration reaching an extraction accuracy of 96.5% and a final composite score of 84.26. Additional analysis reveals significant improvements in extraction completeness, reduction in false positives and false negatives, and effective reuse of a compact set of robust schemas. Error analysis indicates that the primary challenges are associated with noisy HTML structures and incorrect DOM (Document Object Model) element selection, rather than deficiencies in textual content. The findings confirm that combining lightweight transformer models with adaptive memory and schema reuse mechanisms enables the development of scalable, robust, and high-performance web extraction systems. The proposed approach is particularly suitable for real-time information retrieval in safety-critical domains, where timely and accurate data aggregation from heterogeneous sources is essential. Full article

► Show Figures

12 pages, 1154 KB

Open AccessArticle

Non-Standard Squat Posture Detection Method Using Human Skeleton

by **Leiyue Yao**, **Zhiqiang Dai** and **Keyun Xiong**

Abstract

Squats are essential for assessing lower limb strength. However, performing them incorrectly without professional guidance often leads to sports injuries. Currently, most detection methods rely heavily on deep neural networks and massive datasets. This approach brings several downsides. It involves high data labeling [...] Read more.

Squats are essential for assessing lower limb strength. However, performing them incorrectly without professional guidance often leads to sports injuries. Currently, most detection methods

rely heavily on deep neural networks and massive datasets. This approach brings several downsides. It involves high data labeling costs and heavy computing demands. It is also difficult to achieve low-latency feedback on mobile devices. Furthermore, these models often lack robustness when dealing with individual body differences. To tackle these issues, we propose a new real-time squat detection method. Our approach is built on prior rules and statistical models. Here is how it works. First, we use MediaPipe to track the body's skeleton joints in real-time from video feeds, calculating the hip and knee angles frame by frame. Next, we build a hip-knee coordination model using linear regression. This step helps us measure how these joints move together dynamically. Finally, we verify the squat depth using a geometry-based tolerance mechanism. This feature accounts for measurement noise and natural body variations, allowing us to accurately judge if the overall posture is standard. We tested our approach on three different squat styles. The results show that our method catches improper forms quickly and efficiently in real time, achieving an accuracy of 90%. Full article

26 pages, 3180 KB

Open AccessArticle

A Language for Modeling Declarative Knowledge Bases in the Context of Model-Driven Engineering

by **Aleksandr Yurin** and **Nikita Dorodnykh**

Abstract

End-user development (EUD) and model-driven engineering (MDE) are particularly valuable for building classical intelligent systems that rely on declarative knowledge bases. In these knowledge bases, the key dependencies of the domain can be described in the form of logical rules. The general-purpose modeling [...] Read more.

End-user development (EUD) and model-driven engineering (MDE) are particularly valuable for building classical intelligent systems that rely on declarative knowledge bases. In these knowledge bases, the key dependencies of the domain can be described in the form of logical rules. The general-purpose modeling language used in MDE, specifically UML, enables modeling of static data structures and the dynamics of object behavior; however, it does not primarily support the modeling logical rules. In this paper, we propose a rule visual modeling language inspired by UML—Rule Visual Modeling Language (RVML)—which expands the capabilities of MDE in terms of using domain-specific visual languages. This approach substantially supports end-users in constructing declarative knowledge bases. We present the formal semantics, visual syntax, and features of RVML, along with two industrial case studies. We empirically evaluate the effectiveness of RVML in development compared to other graphic notations used for modeling logical rules. Our evaluation demonstrates that RVML provides superior expressiveness and better preservation of semantic integrity. Full article

24 pages, 8962 KB

Open AccessArticle

FetalNet 1.0: TOPSIS-Guided Ensemble Learning with Genetic Feature Selection and SHAP Explainability for Fetal Health Classification from Cardiotocography

by **Shweta**, **Neha Gupta**, **Meenakshi Gupta**, **Massimo Donelli**, **Yogita Arora** and **Achin Jain**

Abstract

Fetal health assessment is a crucial aspect of prenatal care, aimed at the early detection of potential complications to ensure optimal outcomes for both mother and child. Traditional methods, such as the visual analysis of cardiotocography (CTG) data by healthcare professionals, are valuable [...] Read more.

Fetal health assessment is a crucial aspect of prenatal care, aimed at the early detection of potential complications to ensure optimal outcomes for both mother and child. Traditional methods, such as the visual analysis of cardiotocography (CTG) data by healthcare professionals, are valuable but often subjective and time-consuming. This work investigates the application of machine learning techniques, with a focus on ensemble learning, to enhance the accuracy and efficiency of fetal health classification based on CTG data. Genetic Algorithm (GA) is employed for optimal feature selection, identifying the most discriminative subset of CTG attributes to improve model performance and reduce computational complexity. We employ a combination of advanced machine learning models, including AdaBoost, Gaussian Naïve Bayes, Decision Tree, k-nearest neighbors (KNN), and Logistic Regression. The top two models were selected based on comprehensive performance metrics using the TOPSIS (Technique for Order Preference by Similarity to Ideal Solution) method. These models were then integrated through ensemble learning approaches, such as stacking, Particle Swarm Optimization (PSO) weighted averaging, and soft voting, to improve prediction reliability. Our proposed stacking ensemble model achieves a remarkable accuracy of 97.9%, demonstrating its potential as a robust, data-driven tool for fetal health monitoring and the early identification of at-risk pregnancies. The results indicate that machine learning can effectively complement traditional fetal health assessment methods by providing an objective framework to support clinical decision-making. Full article

31 pages, 44324 KB

Open AccessArticle

Performance Evaluation of Post-Quantum Digital Signature in QPSK- and 16QAM-Based WDM Communication Systems

by **Duaa J. Khalaf**, **Arwa A. Moosa** and **Tayseer S. Atia**

Abstract

The integration of post-quantum digital signature (PQDS) algorithms into coherent wavelength-division multiplexing (WDM) optical networks introduces a non-negligible cryptographic overhead that fundamentally alters physical-layer performance characteristics. Unlike conventional studies that treat security and transmission independently, this work provides a cross-layer evaluation of PQDS-induced [...] Read more.

The integration of post-quantum digital signature (PQDS) algorithms into coherent wavelength-division multiplexing (WDM) optical networks introduces a non-negligible cryptographic overhead that fundamentally alters physical-layer performance characteristics. Unlike conventional studies that treat security and transmission independently, this work provides a cross-layer evaluation of PQDS-induced payload expansion and its direct impact on coherent optical system behavior under realistic, DSP-aligned conditions. A structured and reproducible evaluation framework is proposed to systematically analyze this interaction across multiple transmission scenarios, ranging from a single-channel QPSK baseline to a 16-channel WDM system employing both QPSK and 16QAM modulation formats. Key system parameters—including launch power, local oscillator power, bit rate, and fiber length—are jointly optimized, while performance is rigorously assessed in terms of bit error rate (BER), Q-factor, and maximum transmission reach. The results demonstrate a clear performance degradation trend driven by both spectral efficiency scaling and cryptographic payload expansion. The single-channel QPSK system achieves a maximum reach of 203 km, which decreases to 194 km in the 16-channel WDM QPSK configuration due to inter-channel interference and nonlinear effects. In contrast, the 16-channel WDM 16QAM system exhibits a significantly reduced reach of 103 km, reflecting its heightened sensitivity to noise, chromatic dispersion, and fiber nonlinearities. Furthermore, increased payload size associated with PQDS schemes is shown to exacerbate

transmission impairments by extending frame duration and intensifying inter-channel interactions. These findings identify PQDS-induced overhead as a critical system-level constraint that directly governs transmission efficiency, scalability, and performance limits. The study highlights the necessity of cross-layer co-design strategies, where cryptographic mechanisms and physical-layer parameters are jointly optimized to enable efficient, reliable, and quantum-safe coherent optical communication systems. Full article

17 pages, 2551 KB

Open AccessArticle

Generative AI for Education in Infrastructure Systems: Lessons from a BIM-Based Rule-Checking

by **Islem Sahraoui**, **Kinam Kim**, **Lu Gao**, **Zia Ud Din** and **Ahmed Senouci**

Abstract

This study investigates the educational potential of Large Language Models (LLMs) for automating rule-checking tasks in Building Information Modeling (BIM) instruction. A quasi-experimental classroom implementation was conducted over two consecutive semesters with 55 graduate students in a Construction Management program. In Fall 2024, [...] Read more.

This study investigates the educational potential of Large Language Models (LLMs) for automating rule-checking tasks in Building Information Modeling (BIM) instruction. A quasi-experimental classroom implementation was conducted over two consecutive semesters with 55 graduate students in a Construction Management program. In Fall 2024, students were taught manual rule-checking techniques, whereas in Spring 2025, students received additional instruction in LLM-based prompting and Python code generation for automated compliance checking. A mixed-methods evaluation was conducted using surveys, NASA Task Load Index ratings, assignment-based learning outcomes, and structured interviews. Compared with the manual-only cohort, the LLM-assisted cohort reported significantly lower mental, temporal, and frustration demands, as well as higher perceived time efficiency and overall effectiveness. The LLM-assisted group also achieved significantly higher performance in violation detection and method accuracy, although no significant differences were observed in code interpretation or reflective analysis. Qualitative findings further revealed both the efficiency benefits of AI-assisted automation and persistent challenges related to prompt refinement, debugging, and output validation. These findings suggest that LLMs can enhance BIM instruction when paired with structured pedagogical scaffolding to support critical oversight and novice learners. Full article

► Show Figures

25 pages, 2145 KB

Open AccessArticle

AIGU-DPFL: Adaptive Differentially Private Federated Learning with Importance-Based Gradient Updates

by **Fangfang Shan**, **Zhuo Chen**, **Yifan Mao**, **Yuhang Liu**, **Lulu Fan** and **Yanlong Lu**

Computers **2026**, *15*(5), 288; https://doi.org/10.3390/computers15050288 (registering DOI) - 1 May 2026

Abstract

Federated learning, a decentralized machine learning framework, allows multiple participants to jointly train models while keeping their raw data local and unshared. Nevertheless, during the exchange of model updates, the communicated information can still introduce privacy vulnerabilities and potentially result in the exposure [...] Read more.

Federated learning, a decentralized machine learning framework, allows multiple participants to jointly train models while keeping their raw data local and unshared. Nevertheless, during the exchange of model updates, the communicated information can still introduce privacy vulnerabilities and potentially result in the exposure of user data. Over the past few years, differential privacy methods have been broadly incorporated into federated learning frameworks to strengthen the protection of sensitive data. Nevertheless, the noise required to satisfy differential privacy guarantees often causes significant degradation in model performance. Prior studies have typically employed a fixed noise-injection strategy following gradient clipping. Although such methods provide privacy protection, they overlook the varying importance of different gradient dimensions, resulting in noise being injected into unimportant or redundant parameters, thereby causing unnecessary performance loss. To address these limitations, we propose an adaptive differentially private federated learning scheme with importance-based gradient updates (AIGU-DPFL). Specifically, we focus on coordinates with high information content and introduce an adaptive noise injection mechanism, which perturbs gradient updates to satisfy differential privacy guarantees while dynamically controlling noise intensity, thereby achieving sparse and noise-effective gradient updates. AIGU-DPFL markedly enhances the training effectiveness of federated learning models. Comprehensive evaluations conducted on real-world datasets indicate that the proposed method achieves superior performance compared to existing differentially private federated learning techniques. Full article

► Show Figures

16 pages, 361 KB

Open AccessArticle

On-Device Transformer Architectures for Speech Evaluation in Neurodegenerative Disease Detection

by **Lara Marie Reimer**, **Leonard Pries**, **Florian Schweizer**, **Leon Nissen** and **Stephan M. Jonas**

Abstract

Speech alterations are early markers of neurodegenerative diseases. Transformer-based speech models such as Whisper have advanced automated speech assessment, but most systems rely on cloud-based computation, raising privacy concerns. On-device processing could offer a scalable and privacy-preserving alternative. This research's objective was to [...] Read more.

Speech alterations are early markers of neurodegenerative diseases. Transformer-based speech models such as Whisper have advanced automated speech assessment, but most systems rely on cloud-based computation, raising privacy concerns. On-device processing could offer a scalable and privacy-preserving alternative. This research's objective was to evaluate whether a fully on-device speech analysis pipeline can achieve competitive accuracy in detecting Alzheimer's disease and to quantify the contributions of acoustic, linguistic, and embedding features. Therefore, we developed an iOS application running all components, including acoustic analysis, two transformer-based speech-to-text modules (WhisperBase and quantized CrisperWhisper), linguistic feature extraction, and embedding generation, directly on the device. Using the ADReSS Challenge 2020 dataset (N = 156), we trained classical machine-learning classifiers across 20 configurations and evaluated them via a stratified 10-fold cross-validation. Area under the receiver operating curve (AUC), accuracy, precision, recall, and F1 scores were used as performance metrics. An ablation study examined the relevance of each feature group. The best-performing setup (Random Forest with CrisperWhisper transcription and Apple embeddings) achieved an accuracy of 85.4% and an AUC of 0.85. Performance was 5–7% below benchmark

models relying on manual transcripts or server-based processing. Embedding features provided the strongest individual contribution, but the highest accuracy required combining acoustic, linguistic, and embedding information. A fully on-device pipeline for Alzheimer's disease detection from speech is feasible and achieves competitive accuracy while maintaining strict data privacy. These findings highlight the potential of on-device transformer architectures for scalable, privacy-preserving digital screening. Future work should validate the approach in larger and more diverse cohorts. Full article

14 pages, 1377 KB

Open AccessArticle

Multi-Centre Liver Tumour Classification via Federated Learning: Investigating Data Heterogeneity, Transfer Learning, and Model Efficiency

by **Degang Zhu**, **Shiqi Wei** and **Xinming Zhang**

Abstract

This paper investigates federated multi-centre liver tumour classification from contrast-enhanced CT under realistic data heterogeneity and domain shift. To address the practical constraint that medical data are often siloed across institutions, we develop a FedProx-based federated learning pipeline that enables collaborative training without [...] Read more.

This paper investigates federated multi-centre liver tumour classification from contrast-enhanced CT under realistic data heterogeneity and domain shift. To address the practical constraint that medical data are often siloed across institutions, we develop a FedProx-based federated learning pipeline that enables collaborative training without exchanging raw patient data. Using the LiTS dataset as the training domain, we construct a slice-level binary classification task based on voxel-level annotations, while rigorously assessing out-of-distribution generalisation on an external held-out dataset, 3D-IRCADb. We conduct comprehensive experiments across multiple backbone architectures, including ResNet-50, EfficientNet-B3, ViT-B/16, and MobileNetV3-Small, comparing FedProx and FedAvg under three heterogeneity intensities (IID, mild non-IID, and severe non-IID). Furthermore, we evaluate transfer learning strategies, ranging from frozen backbones to partial fine-tuning of the last stage, and perform ablations on the proximal coefficient

μ

and local epochs E to characterise optimisation behaviour. Our results show that FedProx is generally comparable to FedAvg, with slightly more stable behaviour in some heterogeneous settings. We also observe a clear validation-to-external gap, indicating that external-domain robustness remains challenging and requires cautious interpretation for deployment. ImageNet pretraining yields consistent gains, particularly for data-sparse clients, while partial fine-tuning enhances adaptation to CT-specific features. Finally, MobileNetV3-Small offers a favourable performance–efficiency trade-off by reducing communication payload and computation cost, supporting practical deployment on resource-constrained clinical edge devices. Full article

► Show Figures

18 pages, 533 KB

Open AccessArticle

A Rigorous Comparative Study of Supervised Machine Learning Techniques for Network Anomaly Detection: Empirical Insights from the UNSW-NB15 Dataset

by **Nouf Alkhater**

Abstract

The increasing complexity of modern network infrastructures has intensified the need for reliable and efficient intrusion detection systems. While advanced deep learning approaches have demonstrated strong performance, their high computational cost and limited interpretability restrict their practical deployment in real-time environments. This study [...] Read more.

The increasing complexity of modern network infrastructures has intensified the need for reliable and efficient intrusion detection systems. While advanced deep learning approaches have demonstrated strong performance, their high computational cost and limited interpretability restrict their practical deployment in real-time environments. This study presents a systematic empirical evaluation of four supervised machine learning models—Decision Tree, Random Forest, Support Vector Machine (SVM), and XGBoost—for network anomaly detection using the UNSW-NB15 dataset. To ensure methodological rigor, a structured preprocessing pipeline and a five-fold stratified cross-validation framework were employed. Model performance was assessed using multiple evaluation metrics, including accuracy, precision, recall, F1-score, and area under the ROC curve (AUC). In addition, a feature importance analysis was conducted to identify the most influential network traffic attributes contributing to anomaly detection. The results show that ensemble-based methods outperform individual classifiers, with XGBoost achieving the best overall performance (accuracy = 0.97, AUC = 0.98) along with high stability across validation folds. The analysis further reveals that a subset of flow-based and temporal features—such as sttl, sload, and dload—plays a critical role in distinguishing between normal and malicious traffic. This study provides a rigorous, interpretable, and reproducible benchmarking framework for supervised machine learning in network anomaly detection. The findings provide practical insights for developing efficient and scalable intrusion detection systems suitable for real-world deployment. Full article

► Show Figures

Highly Accessed Articles

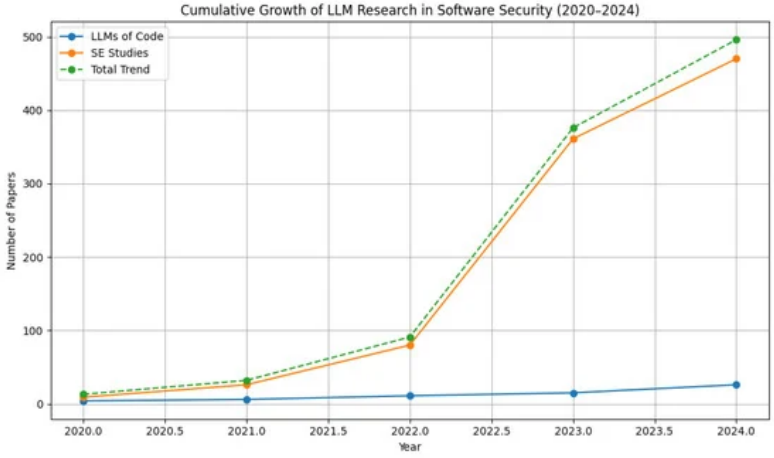

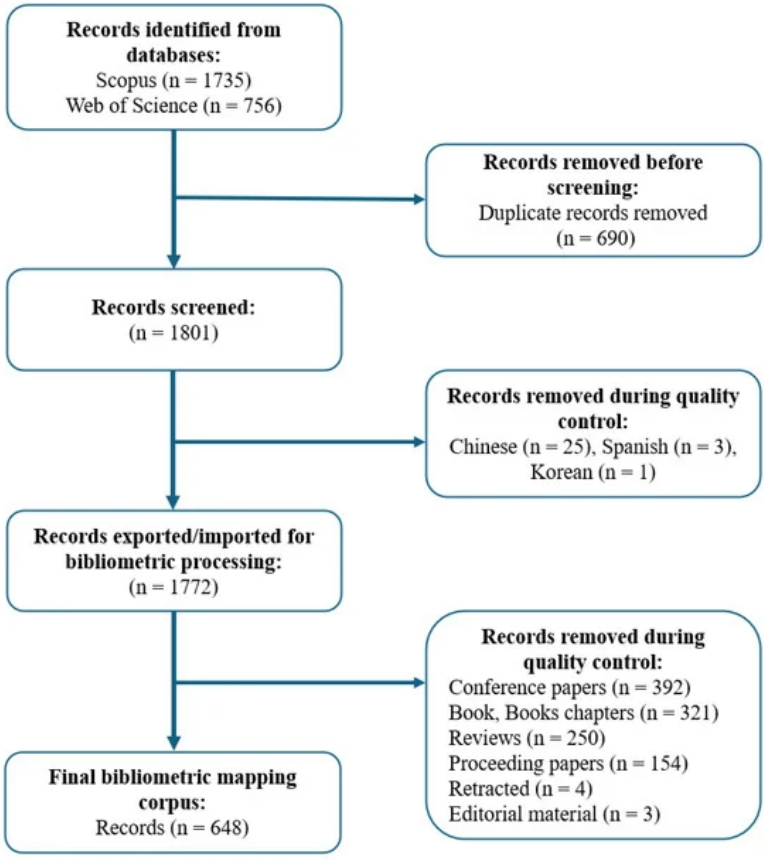
Records identified from databases:
Scopus (n = 1735)
Web of Science (n = 756)
Records removed before screening:
Duplicate records removed (n = 690)
Records screened:
(n = 1801)
Records removed during quality control:
Chinese (n = 25), Spanish (n = 3), Korean (n = 1)
Records exported/imported for bibliometric processing:
(n = 1772)
Records removed during quality control:
Conference papers (n = 392)
Book, Books chapters (n = 321)
Reviews (n = 250)
Proceeding papers (n = 154)
Retracted (n = 4)
Editorial material (n = 3)
Final bibliometric mapping corpus:
Records (n = 648)

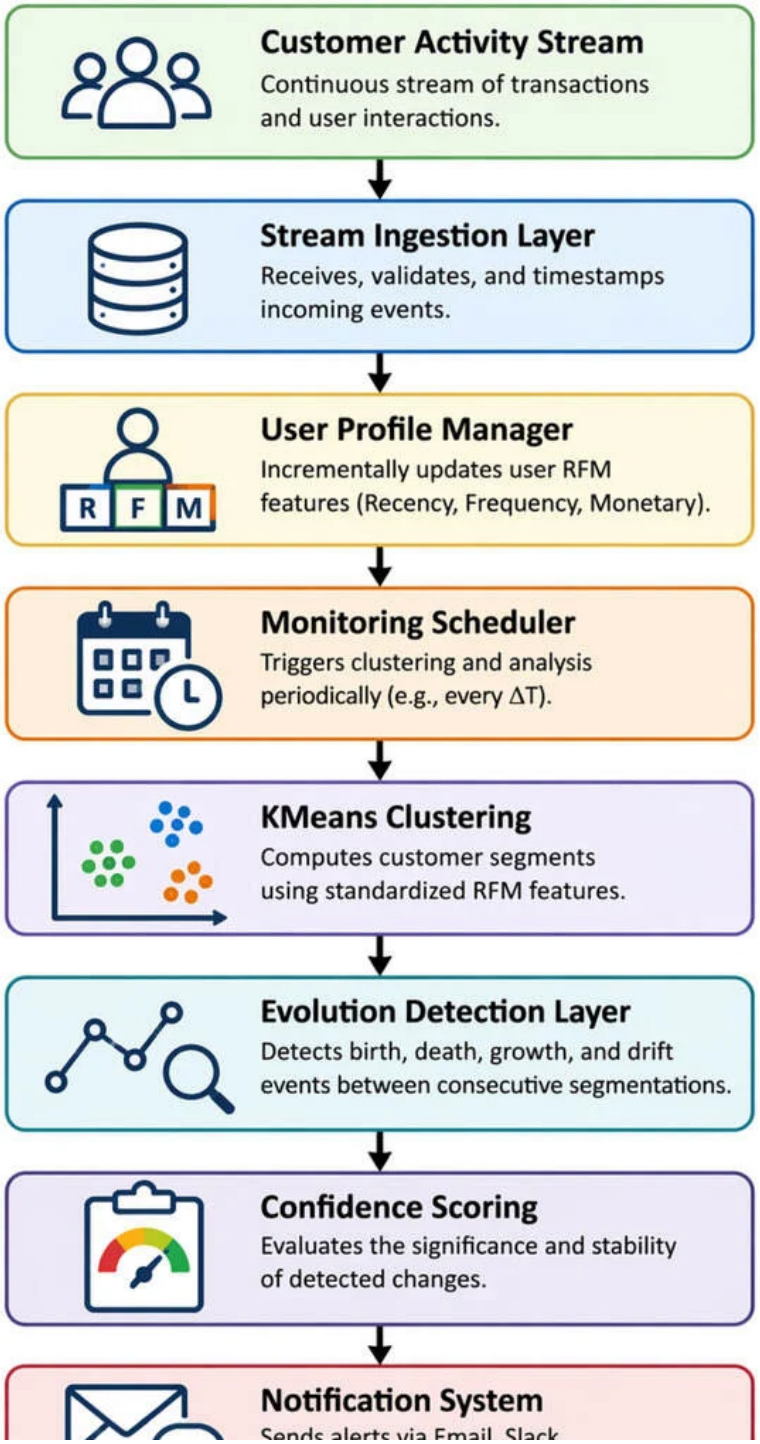
Customer Activity Stream
Continuous stream of transactions and user interactions.
Stream Ingestion Layer
Receives, validates, and timestamps incoming events.
R F M
User Profile Manager
Incrementally updates user RFM features (Recency, Frequency, Monetary).
Monitoring Scheduler
Triggers clustering and analysis periodically (e.g., every ΔT).
KMeans Clustering
Computes customer segments using standardized RFM features.
Evolution Detection Layer
Detects birth, death, growth, and drift events between consecutive segmentations.
Confidence Scoring
Evaluates the significance and stability of detected changes.
Notification System

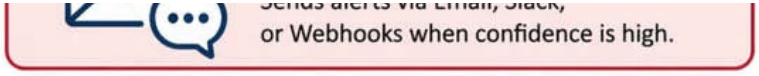

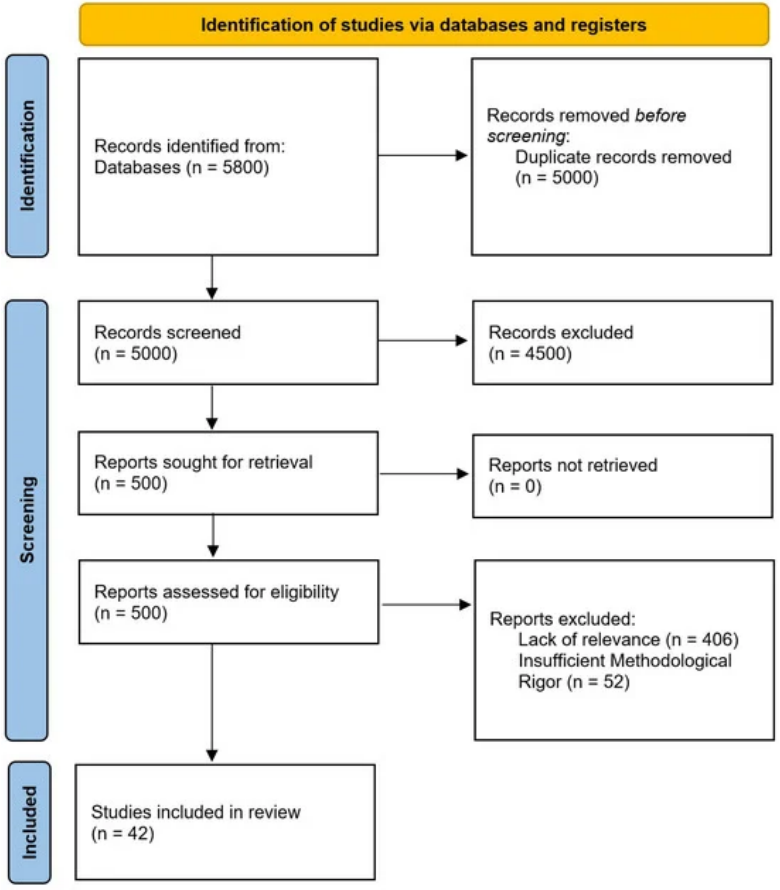

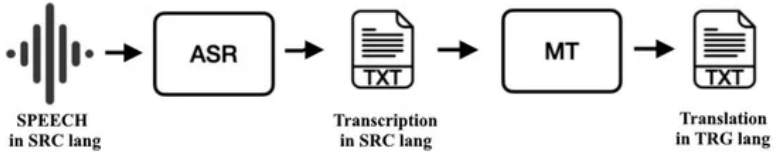

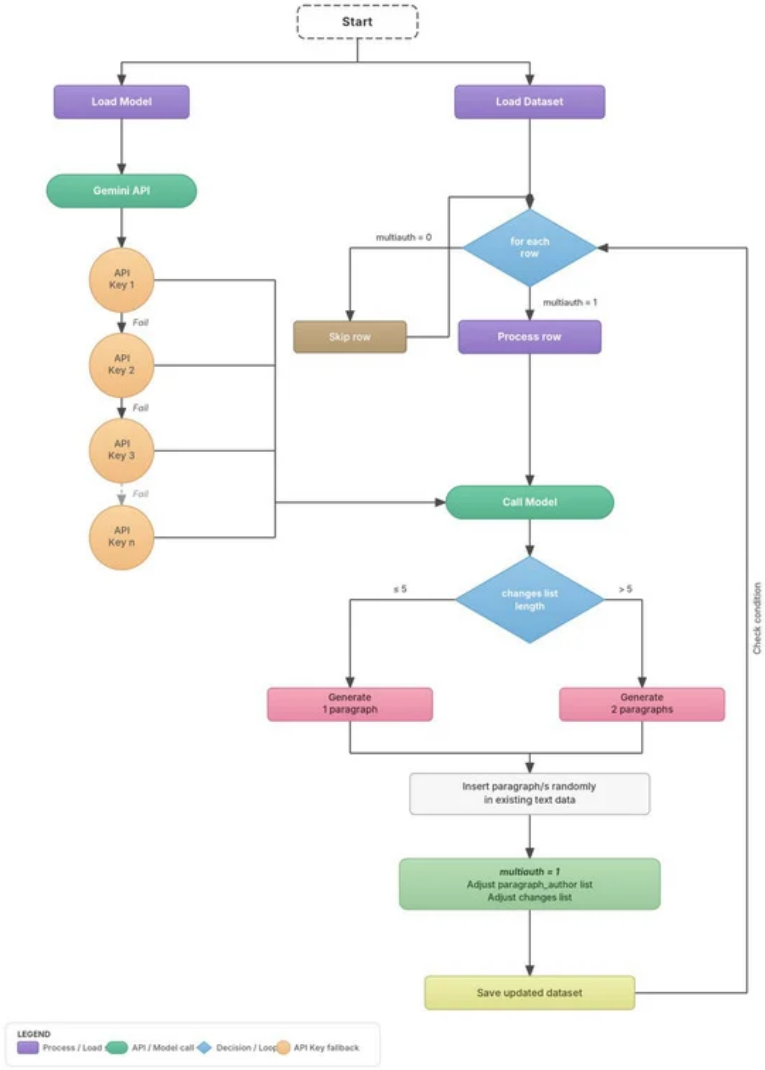

Topics

Topic in AI, Computers, Education Sciences, Societies, Future Internet, Technologies

AI Trends in Teacher and Student Training Topic Editors: José Fernández-Cerero, Marta Montenegro-Rueda
Deadline: 11 July 2026

Conferences

Special Issues

Computers

Logical OperatorOperator

Search Text

Search Type

add_circle_outline

remove_circle_outline

Editorial Board

Please note that the order in which the Editors appear on this page is alphabetical, and follows the structure of the editorial board presented on the MDPI website under information for editors: editorial board responsibilities.

Members

Prof. Dr. Paolo Bellavista

Website
Editor-in-Chief

Department of Computer Science & Engineering (DISI), University of Bologna, 40136 Bologna, Italy
Interests: wireless sensor and actuator networks; middleware for sensor and actuator networks; vehicular sensor networks; edge computing; fog computing; online stream processing of sensing dataflows; IoT and big data processing; pervasive and mobile computing; cooperative networking; cyber physical systems for Industry 4.0
Special Issues, Collections and Topics in MDPI journals


Prof. Dr. Leandros Maglaras

*

Website

Section Editor-in-Chief

School of Computing, Edinburgh Napier University, Edinburgh EH10 5DT, UK
Interests: critical infrastructure security; IoT security & privacy; intrusion detection systems; incident response
* Section: ICT Infrastructures for Cybersecurity
Special Issues, Collections and Topics in MDPI journals


Prof. Dr. Wenbing Zhao

Website

Associate Editor

Department of Electrical Engineering and Computer Science, Cleveland State University, Cleveland, OH 44115, USA
Interests: human-centered systems; machine learning; data science; distributed computing; blockchain
Special Issues, Collections and Topics in MDPI journals


Dr. AbdulRahman Alsewari

Website

Editorial Board Member

School of Computing and Digital Technology, Faculty of Computing, Engineering and the Built Environment, Birmingham City University, Birmingham B4 7XG, UK
Interests: artificial intelligence; machine learning; software engineering; optimization; software testing
Special Issues, Collections and Topics in MDPI journals


Dr. Mostafa Rahimi Azghadi

Website
Editorial Board Member

College of Science & Engineering, James Cook University, Townsville City QLD 4814, Australia
Interests: neuromorphic engineering; spiking neural networks; memristors and memristive systems; very lage scale Integration (VLSI) design; embedded systems; quantum cellular automata
Special Issues, Collections and Topics in MDPI journals


Dr. Silvia Biasotti

Website
Editorial Board Member

Istituto di Matematica Applicata e Tecnologie Informatiche, Consiglio Nazionale delle Ricerche, 16149 Genova, Italy
Interests: geometric modelling; shape analysis; 3D shape recognition and classification
Special Issues, Collections and Topics in MDPI journals

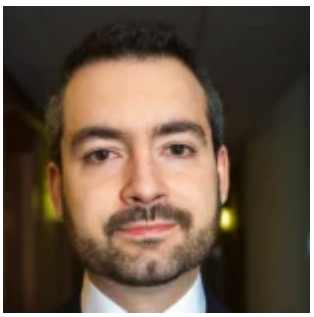
Prof. Dr. Fernando Bobillo

Website

Editorial Board Member

Department of Computer Science and Systems Engineering, Ada Byron Building (School of Engineering and Architecture), University of Zaragoza, Zaragoza, Spain

Interests: semantic web; fuzzy logic; knowledge representation; reasoning; mobile computing

Special Issues, Collections and Topics in MDPI journals

Dr. Paul Bogdan

Website1 Website2

Editorial Board Member

Ming Hsieh Department of Electrical Engineering, University of Southern California, 3740 McClintock Ave., Los Angeles, CA 90089-2563, USA

Interests: analysis and optimization of embedded systems; systems-on-chip/network-on-chip; low-power VLSI systems; theoretical foundations of cyber-physical systems; molecular communication; modeling and optimization of biologically propelled micro-robotic swarms; control of fractal dynamics

Special Issues, Collections and Topics in MDPI journals

Dr. M. Ali Akber Dewan

Website

Editorial Board Member

School of Computing and Information Systems, Faculty of Science and Technology, Athabasca University, Athabasca, AB T9S 3A3, Canada

Interests: image processing; computer vision; machine learning; pattern recognition; adaptive biometrics; artificial intelligence; medical image analysis

Special Issues, Collections and Topics in MDPI journals

Dr. Anind Dey

Website

Editorial Board Member

Information School, University of Washington, Seattle, WA 98105, USA

Interests: human-computer interaction; ubiquitous and pervasive computing; software toolkits

Dr. Javier Diaz-Montes

Website

Editorial Board Member

Rutgers Discovery Informatics Institute (RDI2), Rutgers University, 96 Frelinghuysen Road, Piscataway, NJ 08854, USA

Interests: cloud computing; autonomic computing; virtualization; middleware; scheduling

Prof. Dr. Jack Dongarra

Website

Editorial Board Member

Innovative Computing Laboratory, EECS Department, 1122 Volunteer Blvd, University of Tennessee, Knoxville, TN 37996-3450, USA

Interests: parallel computing; mathematical software; linear algebra; performance evaluation

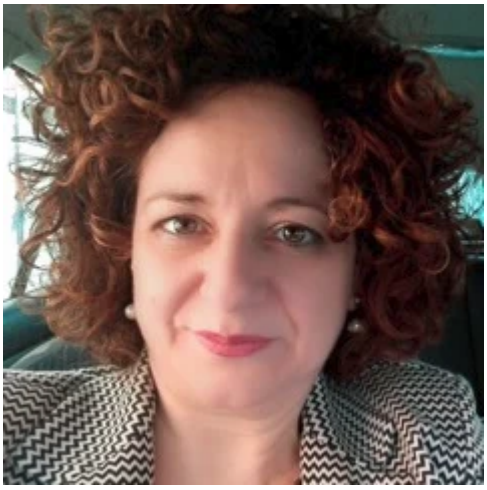

Prof. Dr. Anna Rita Fasolino

Website

Editorial Board Member

Department of Electrical Engineering and Information Technology (DIETI), University of Naples Federico II, 80138 Napoli, Italy

Interests: software engineering; software testing; software maintenance; reverse engineering; mobile application testing; software quality

Special Issues, Collections and Topics in MDPI journals


Dr. Martin Fleury

Editorial Board Member

School of Science, Technology and Engineering, University of Suffolk, Ipswich IP4 1QJ, UK
Interests: multimedia networks; wireless; video communication over wireless networks; multimedia network security
Special Issues, Collections and Topics in MDPI journals


Dr. Anuroop Gaddam

Website
Editorial Board Member

School of Information Technology, Deakin University, Melbourne 3125, Australia
Interests: internet of things (IoT); designing and developing IoT based monitoring system for health informatics; developing machine learning techniques for sensor faults, outlier detection & predictive analysis; designing & developing smart sensors; wireless sensor network; smart homes for elder care


Dr. Ann Gordon-Ross

Website
Editorial Board Member

Department of Electrical and Computer Engineering, University of Florida, Gainesville, FL 32611, USA
Interests: computer engineering; low-power design; embedded systems; reconfigurable computing; platform design; aerospace system; fault tolerance; dynamic optimizations; hardware

design; real-time systems; computer architecture; multi-core platforms
Special Issues, Collections and Topics in MDPI journals


Dr. Paul Grace

Website
Editorial Board Member

Computer Science, Aston University, Birmingham B4 7ET, UK
Interests: middleware; distributed systems; autonomic computing; cybersecurity; privacy engineering


Dr. Sabine Graf

Website
Editorial Board Member

School of Computing and Information Systems, Faculty of Science and Technology, Athabasca University, 1200, 10011-109 Street, Edmonton, AB T5J3S8, Canada
Interests: user/learner modelling, adaptive and personalized systems, learning/academic analytics, educational data mining, artificial intelligence in education, technology enhanced learning

Dr. Margaret Hamilton

Website

Editorial Board Member

School of Computer Science and Information Technology, RMIT University, Melbourne, VIC 3000, Australia
Interests: software engineering in mobility, modelling, testing, ethnographic action research; computer science education including new technologies, problem-based learning, work-integrated learning and academic integrity

Prof. Dr. Hovhannes Harutyunyan

Website
Editorial Board Member

Department of Computer Science and Software Engineering, Concordia University, Montreal, QC H3G 1M8, Canada
Interests: combinatorics of networks; algorithmic graph theory; parallel and distributed algorithms
Special Issues, Collections and Topics in MDPI journals


Prof. Dr. Reiko Heckel

Website
Editorial Board Member

Department of Informatics, University of Leicester, Leicester LE1 7RH, UK
Interests: graph transformation theory and application; model-based software engineering; formal models for service-oriented and P2P architectures; stochastic modelling and analysis of dynamic networks (social, biological and technical)


Prof. Dr. Michail Kalogiannakis

Website
Editorial Board Member

Department of Special Education, University of Thessaly, Argonafton & Filellinon, 38221 Volos, Greece
Interests: quantitative methods in science education; the integration of digital technologies (e.g., gamification, mobile learning); assessment in STEM education; the application of artificial intelligence in science teaching
Special Issues, Collections and Topics in MDPI journals


Dr. Hyunbum Kim

Website
Editorial Board Member

Department of Embedded Systems Engineering, Incheon National University, Incheon 22012, Republic of Korea
Interests: AI-driven Internet of Things; intelligent computing; virtual emotion system;

unmanned aerial vehicles; smart cities; next generation systems; cyber security

Prof. Dr. Akhil Kumar

Website
Editorial Board Member

Smeal College of Business, Pennsylvania State University, University Park, PA 16802, USA
Interests: blockchain technology; business analytics; deep learning; health IT and healthcare forums; BPM and workflow systems; process mining

computers

MDPI

Article

Adaptive Optimization of Diffuse Spot Intensities and Locations for Enhanced Performance in Indoor Visible-Light Optical Wireless Communications

Michael David [1], Abdullahi. B. Babadoko [1,2], Suleiman Zubair [1], Abraham U. Usman [1], Abraham. D. Morakinyo [3], Stephen S. Oyewobi [1] and Topside E. Mathonsi [4,*]

[1] Department of Telecommunications Engineering, Federal University of Technology, P.M.B. 65, Bosso, Minna 920101, Niger State, Nigeria; mikeforheaven@futminna.edu.ng (M.D.); babadoko.pg915977@st.futminna.edu.ng (A.B.B.); zubairman@futminna.edu.ng (S.Z.); usman.abraham@futminna.edu.ng (A.U.U.); oyewobistephen@futminna.edu.ng (S.S.O.)
[2] Technology Incubation Centre (TIC), National Board for Technology Incubation, Federal Ministry of Innovation, Science and Technology, Minna 910001, Niger State, Nigeria
[3] Department of Industrial Design, Modibbo Adama University, Yola 640001, Adamawa State, Nigeria; morakinyo@mau.edu.ng
[4] Department of Information Technology, Tshwane University of Technology, Pretoria 0001, South Africa
* Correspondence: mathonsite@tut.ac.za

Abstract

This study explores the application of JAYA optimization algorithms to significantly enhance the performance of indoor optical wireless communication (OWC) systems. By strategically optimizing photo-signal parameters, the system was able to improve signal distribution and reception within a confined space using circular and randomly positioned diffuse spots. The primary objective was to maximize signal-to-noise ratio (SNR) and minimize delay spread (DS), two critical factors that affect transmission quality in OWC systems. Given the challenges posed by background noise and multipath dispersion, an effective optimization strategy was essential to ensure robust signal integrity at the receiver end. Key achievements of JAYA optimization include significant performance gains, such as a 29% improvement in SNR, enhancing signal clarity and reception, and a 23.3% reduction in delay spread, ensuring stable and efficient transmission. System stability also improved, with the standard deviation of SNR improving by up to 5%, leading to a more consistent performance, while the standard deviation of delay spread improved by up to 9.9%, minimizing variations across receivers. Resilience against environmental challenges: Optimization proved effective even in the presence of ambient light noise and complex multipath dispersion effects, reinforcing its adaptability in real-world applications. The findings of this study confirm that JAYA optimization algorithms offer a powerful solution for overcoming noise and dispersion issues in indoor OWC systems, leading to more reliable and high-quality optical wireless communications. These results underscore the importance of algorithmic precision in enhancing system performance, paving the way for further advancements in indoor optical networking technologies.

Keywords: delay spread; communication; diffuse spot; signal-to-noise ratio; JAYA

Academic Editor: Paolo Bellavista

Received: 9 September 2025
Revised: 23 October 2025
Accepted: 26 October 2025
Published: 9 December 2025

Citation: David, M.; Babadoko, A.B.; Zubair, S.; Usman, A.U.; Morakinyo, A.D.; Oyewobi, S.S.; Mathonsi, T.E. Adaptive Optimization of Diffuse Spot Intensities and Locations for Enhanced Performance in Indoor Visible-Light Optical Wireless Communications. *Computers* **2025**, *14*, 537. https://doi.org/10.3390/computers14120537

1. Introduction

In recent years, the demand for high-speed data transmission has surged exponentially, driven by the expansion of digital services, cloud computing, and the Internet of

Things (IoT). Traditional radio frequency (RF) communication systems, operating within the congested spectrum of 3 kHz to 300 GHz, face increasing limitations, struggling to accommodate the ever-growing data demands. Despite advancements in signal processing and modulation techniques, the saturation of RF bands presents a formidable challenge to future wireless systems [1].

In response to these constraints, optical wireless communication (OWC) systems have emerged as a promising alternative, offering access to a largely unexploited spectrum capable of delivering data rates from tens of gigabits per second (Gbps) to terabits per second (Tbps) [2]. OWC systems, particularly those designed for indoor environments, present unique advantages such as unlicensed spectrum usage, immunity to RF interference, and enhanced security. However, they are also prone to challenges, including intersymbol interference, background noise due to ambient lighting, and power constraints imposed by skin and eye safety regulations [3].

The ongoing transition to fifth-generation (5G) and the anticipated rollout of sixth-generation (6G) wireless networks demand solutions that address the limitations of RF communication. The saturation of RF channels reduces data transfer efficiency and increases latency, leading researchers to explore hybrid solutions integrating RF and Visible-Light Communication (VLC) systems [4]. Indoor OWC networks, while offering high data rates and frequency reuse capabilities, still face critical performance challenges related to signal degradation and multipath dispersion. One key aspect influencing system efficiency is the positioning and intensity distribution of diffuse spots, which play a significant role in optimizing signal-to-noise ratio (SNR) and delay spread (DS) [5]. This research aims to improve data transmission rates by optimizing the intensities and spatial distribution of diffuse spots using hybrid JAYA and particle swarm optimization (PSO) techniques. Through this approach, enhanced SNR values and minimized delay spread will be achieved, contributing to the advancement of OWC technologies as viable solutions for next-generation wireless communication networks [6].

The surge in demand for high-speed data transmission has propelled the exploration of alternative wireless communication technologies, particularly OWC. Traditional radio frequency (RF) wireless communication systems face bandwidth saturation issues, limiting their ability to meet future network requirements [2]. OWC offers an unlicensed spectrum with potential data rates extending to terabits per second, making it a viable candidate for next-generation communication systems [2].

OWC systems present unique advantages, including high security, immunity to RF interference, and reduced latency [3]. They are ideal for indoor applications where frequency reuse can enhance capacity. However, several challenges persist, including signal corruption due to ambient light, intersymbol interference, and skin/eye safety concerns [5]. Researchers have proposed various approaches, including optimizing diffusion spots' locations and intensities, to mitigate these effects and enhance OWC efficiency [6].

The transition to 5G and 6G networks has necessitated the integration of hybrid optical-RF communication platforms. Studies indicate that merging visible-light communication (VLC) with RF in indoor environments can boost speed and suppress latency concerns [4]. The deployment of hybrid optical-RF solutions optimizes bandwidth usage and improves spectral efficiency [4]. Furthermore, non-line-of-sight (NLOS) configurations have been explored to enhance mobility and data transmission [7].

Researchers have identified the optimization of diffuse spots' locations and intensities as critical to enhancing SNR and reducing DS. The hybrid JAYA/PSO method has been investigated to improve transmission efficiency, showing significant advancements in achieving high bit rates with lower complexity and cost [8]. These optimization techniques help overcome multipath propagation losses and enhance system reliability [9].

The integration of organic semiconductors into VLC technologies offers promising results for achieving efficient white-light communication links [6]. As OWC systems continue evolving, innovative solutions such as adaptive modulation schemes and network densification strategies will be key to supporting the rapid growth of wireless data traffic [10].

2. Optimization in Optical Wireless Communication Systems

OWC systems have seen significant advancements through various optimization techniques aimed at enhancing performance. Previous approaches have tackled different aspects of system refinement, yet certain critical factors remain unaddressed. For instance, while genetic algorithms have been employed to regulate optical wireless channels, they often overlook DS in their fitness functions [3]. Similarly, divide-and-conquer strategies have successfully adapted transmitter characteristics [11], and simulated annealing has fine-tuned spot patterns in diffuse OWC links, improving DS and received power standard deviation, yet spot intensities were not considered. Even efforts focused on optimizing diffuse spot center dispersion have left intensity variations unexplored [3].

This study introduces the JAYA optimization technique as a holistic solution, simultaneously refining both the positioning and intensity distribution of diffuse spots. By prioritizing SNR enhancement and DS minimization, our approach ensures superior performance while accounting for multipath dispersion and background noise. Various optimization scenarios are examined to reveal their impact on system efficiency, with results benchmarked against a baseline model featuring a circular arrangement of equal-intensity spots centered on receivers. The proposed channel model and optimization algorithm pave the way for adaptable and high-performing OWC systems across diverse indoor environments.

3. Optical Wireless Communication System Model

This section presents a sophisticated model of an indoor OWC system, as depicted in Figure 1. The setup comprises key components, including transmitters (Tx), receivers (Rx), noise sources, and a dynamic feedback loop, each playing a crucial role in signal transmission and optimization.

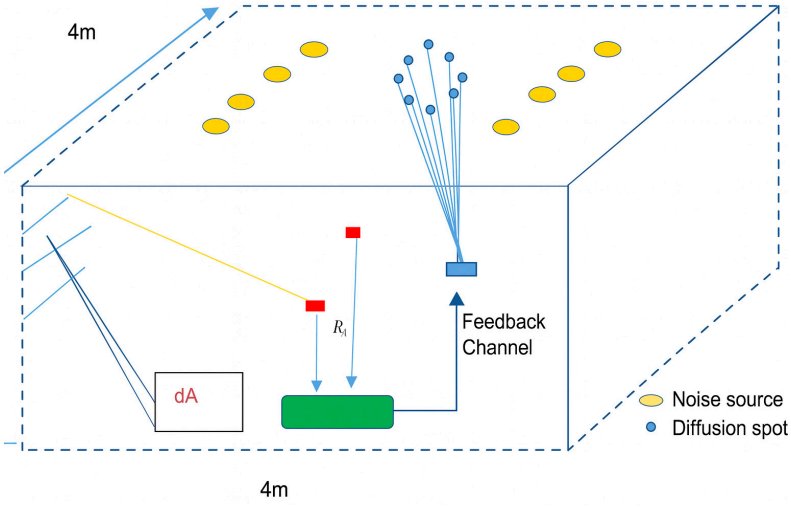

Figure 1. Showing the indoor OWC environment considered in this work.

At the core of the system, a single Tx, configured as either a two-dimensional vertical cavity surface-emitting laser diode (VCSEL) or a resonant cavity LED array [5], projects diffuse spots (DiSs) onto the ceiling. These spots effectively function as secondary indepen-

dent transmitters, ensuring robust signal distribution across the environment. The spatial arrangement of these diffuse patterns is highly adaptable, allowing for customization based on the room's dimensions and functional requirements.

A key feature of the system is its adaptive feedback mechanism, which continuously refines DiS locations and intensities to enhance communication efficiency. Given that DiSs exhibit Lambertian reflection characteristics [12], with a reflection coefficient denoted as ρ, only first- and second-order reflections are accounted for in the model. Higher-order reflections are excluded due to their negligible impact on system performance [8].

The system's behavior is mathematically characterized by the channel impulse response, formally expressed in Equation (1) [13]. This equation encapsulates the underlying dynamics of signal propagation, enabling precise analysis of OWC system performance within diverse indoor environments [14].

$$h\left(t : T_f : R_f\right) = \sum_{r=0}^{k} h^r(t : \tau : \mathcal{R}) \tag{1}$$

$$h^r(t : \tau : \mathcal{R}) = P_s \sum_{m=1}^{N_e} \frac{L+1}{2\pi} \frac{cos^L(\varphi_{RT})\cos(\theta_{RT})}{D^2{}_{RT}} \rho A_R \times rect\left(\frac{\theta_{RT}}{FOV_R}\right)\delta\left(t - \frac{D_{RT}}{c}\right) \tag{2}$$

Equation (1) encapsulates the fundamental parameters that define the behavior of an indoor OWC system. Here, L represents the Lambertian order, shaping the distribution of emitted optical power. The transmitted power, P_s, dictates the intensity of the signal, while T_x and R_x mark the initial transmission and final reception points, respectively.

To model the system's impulse response, the parameter t and the delta function characterize the arrival time at the receiver (R_x), relative to an ideal unit impulse radiated at $t = 0$ [7]. The reflection order, r further refines signal propagation, where $r = 0$ corresponds to a direct line-of-sight (LoS) transmission, while higher values denote reflections. The number of reflecting elements, N_e determines the complexity of multipath signal interactions.

A secondary transmission point (T) can be a diffuse spot or a Lambertian reflecting surface, ensuring efficient signal redirection. Similarly, the receiving point (R) may be either a photodetector (PD) or another reflecting surface, impacting signal absorption and redirection. The system's impulse response, $h(t; T; R)$, quantifies reflections up to the *rth* order.

Key physical attributes play crucial roles in signal propagation:

- D_{TR} represents the distance between transmission and reception points.
- A_R is the photosensitive or reflecting element area, affecting signal capture efficiency.
- FOV_R, the PD's field of view, is set at 170° to maximize reception. When the receiving point is a reflecting surface, FOV_R defaults to 1.
- rect(x) serves as a bounding function, equaling 1 for $x \leq 1$ and 0 otherwise.

Additionally, θ_{RT} denotes the angle between D_{TR} and normality at the receiving point (n^R), while φ_{RT} defines the corresponding angle at the transmitting point (n^T). The speed of light, c, governs the fundamental transmission dynamics.

For an intensity modulation/direct detection (IM/DD) OWC system, the received photocurrent follows Equation (3), capturing the interplay of transmitted signal intensity, reflection orders, and environmental influences, essentially defining the system's responsiveness to diverse indoor conditions.

$$(t) = RPD\ x(t) * h\left(t : T_f; R_f\right) + n(t) \tag{3}$$

Equation (3) encapsulates key factors governing optical wireless communication system performance. The responsivity of the photodetector (RPD) determines how efficiently the incoming optical signal is converted into an electrical current. The transmitted signal,

$x(t)$ carries the modulated data, while $n(t)$ introduces additive white Gaussian noise, an inherent challenge in wireless systems that affects signal clarity and detection accuracy.

One of the most critical considerations in wireless communication is DS, which quantifies temporal dispersion in signal reception. It represents the duration over which the energy from an impulse response arrives at the receiver, influencing system reliability and data integrity. Excessive DS can lead to inter-symbol interference, degrading communication quality, especially in high-speed optical networks.

Equation (4) precisely defines S, capturing how multipath propagation impacts signal arrival timing [9]. By understanding and mitigating delay spread, optical wireless systems can optimize their performance, ensuring robust, high-fidelity data transmission in diverse indoor environments:

$$DS = \sqrt{\frac{\int (t-\mu)^2 \left(h\left(t : T_f; R_f\right)\right)^2 dt}{\int \left(h\left(t : T_f; R_f\right)\right)^2 dt}} \tag{4}$$

And μ is the mean delay, which is given by

$$\mu = \frac{\int t\left(h\left(t : T_f; R_f\right)\right)^2 dt}{\int \left(h\left(t : T;_f R_f\right)\right) dt} \tag{5}$$

Note: $h\left(t : T_f;\ R_f\right)$ is the channel impulse response LOS while at a diffuse spot or a Lambertian surface, *rth* reflection order impulse response of : $h_r\left(t : T_f;\ R_f\right)$. The SNR is given in Equation (6) as shown below [15]:

$$SNR = \frac{(RP_\tau)^2}{\sigma^2_{total}} \tag{6}$$

where P_r is the average optical receiver power and σ^2_{total} is the total variance of the noise, which is expressed as follows:

$$\sigma^2_{total} = \sigma^2_{PA} + \sigma^2_{BN} \tag{7}$$

where ${\sigma_{PA}}^2$ is the noise variance of the pre-amplified signal and ${\sigma_{BN}}^2$ is the ambient light noise variance.

OWC leverages three primary modulation schemes: baseband, multicarrier, and multicolor [14]. Each approach serves distinct purposes in optimizing signal transmission and reception. Baseband modulation encompasses techniques such as pulse amplitude modulation (PAM), pulse position modulation (PPM), pulse interval modulation (PIM), and carrier-less amplitude phase (CAP) modulation, all of which are tailored to efficiently encode data while managing signal integrity.

Meanwhile, multicolor modulation, which is often implemented using wavelength division multiplexing (WDM) with blue, green, and red (BGR) LEDs, allows high data rates and multi-user access by transmitting information across separate wavelengths [6]. Although four-color laser diodes (LDs) have demonstrated superior performance compared to conventional three-color LEDs, challenges persist, particularly with white light LEDs, where the phosphor's slow response constrains modulation bandwidth. Overcoming these limitations requires sophisticated signal processing techniques and advanced modulation formats.

Complementing these developments, the JAYA algorithm [5] emerges as a groundbreaking optimization technique, which is applicable to both constrained and unconstrained

problems. Rooted in the principle of achieving the best possible solution while steering clear of the worst, JAYA continuously refines outcomes by dynamically shifting toward optimal configurations. Its name, derived from the Sanskrit word for "victory," aptly reflects its approach to systematic improvement.

A defining strength of JAYA is its parameter-free nature, requiring only population size and iteration count, unlike other algorithms that demand multiple tuning parameters such as inertia weight, learning factors, and acceleration coefficients (e.g., particle swarm optimization). This streamlined methodology significantly simplifies implementation, accelerates computation, and enhances efficiency.

Mathematically, let f(x) represent an objective function with D-dimensional variables $(j = 1, 2, \ldots, D)$. The estimated value of the jth variable for the ith candidate solution is $x_{i,j}$, forming the vector $x_i = (x_i, 1, x_i, 2, \ldots, x_i, D)$ to define the candidate's position in the search space. The best solution, $x_{best} = (x_{best1}, x_{best2}, \ldots, x_{bestD})$, exhibits the highest f(x) value, while the worst solution, $x_{worst} = (x_{worst,1}, x_{worst,2}, \ldots, x_{worst,D})$, represents the least favorable outcome. Equation (8) governs the iterative update of $x_{i,j}$, ensuring the system converges toward the optimal solution.

$$x^f{}_{i,j} = x_{i,j} + rand_1 \cdot \left(x_{best,j} - |x_{i,j}| - rand_2 \cdot \left(x_{worst,j} - |x_{i,j}| \right) \right) \quad (8)$$

Equation (8) plays a pivotal role in the JAYA optimization algorithm, guiding each candidate solution toward optimal performance. Here, x_(best,j) and x_(worst,j) denote the values of the jth variable for the best and worst solutions, respectively. The updated variable, xi,j, represents the newly refined value based on the optimization process, while |xi,j| expresses its absolute magnitude.

A critical component of JAYA is the influence of rand1 and rand2, two randomly generated values uniformly distributed within the range [0, 1]. In Equation (8), the term rand1 (x_(best,j) – x_(worst,j)) directs the solution towards improvement, continuously refining its position within the search space. This mechanism ensures that each iteration prioritizes better solutions, systematically avoiding suboptimal outcomes.

Unlike traditional optimization techniques which require extensive parameter tuning, JAYA adopts a self-sufficient approach, adjusting solutions dynamically. Once a solution is identified, the algorithm moves closer to the best and steers further from the worst, reinforcing the victory-driven nature of JAYA. Through this iterative refinement, the algorithm consistently strives for efficiency and precision, making it a highly effective optimization strategy.

The JAYA algorithm is implemented according to the following steps:

1. Initialize the population size (IPZ), design variables, and fitness function evaluation count (FFE).
2. Assess the fitness function value for each candidate solution.
3. Set FEE = NP (initial evaluation count).
4. While FEE < Max_FEE, repeat the following steps:
   - Select the best candidate (x_{best}) and the worst candidate (x_{worst}) from the population.
   - For i = 1 to NP, evaluate the fitness function value for the updated candidate.
   - Increment FEE = FEE + 1.
   - Accept the new solution only if it outperforms the previous one.
5. End iteration once optimal criteria are met.

By continuously refining each candidate's position, JAYA eliminates reliance on complex parameter tuning, making it an efficient and scalable optimization framework. Whether it is applied to engineering, data science, or machine learning, its ability to max-

imize potential while avoiding poor solutions makes it a standout algorithm for robust decision-making. Figure 2 shows the JAYA algorithm flowchart.

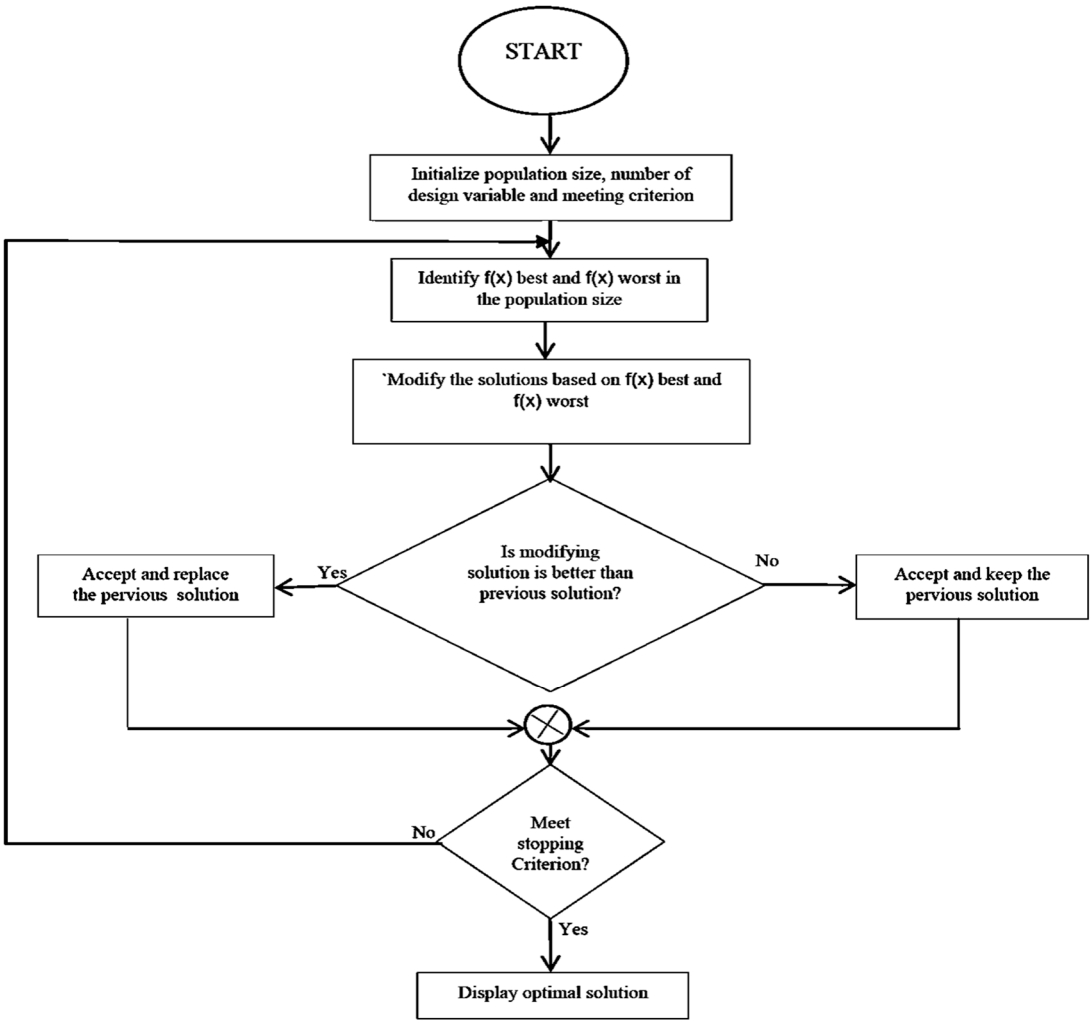

Figure 2. Jaya algorithm flow chart.

4. Results and Discussion

To evaluate system performance, a controlled indoor simulation environment was designed, replicating real-world conditions within a 4 m × 4 m × 3 m room. Receivers were strategically positioned 1 m above the floor, ensuring varied signal propagation pathways.

4.1. Noise and Transmission Sources

Eight Luminous-LED Plyc4545 (PAR38) light-emitting diode lamps (Conglom, Inc. 2600 Avenue Marie-Curie, Montreal, QC, H4S 2C3, Canada) were incorporated as noise sources. With a Lambertian order of 33.1 and an emitted power of 65 W, these sources exhibited highly directive characteristics, significantly influencing system performance. Their high Lambertian order made them more focused than the diffuse spots, reinforcing their role as interference factors.

Simultaneously, eight diffuse spots, functioning as secondary independent transmitters, were implemented to facilitate signal distribution. These spots played a crucial role in adaptive transmission, ensuring robust signal coverage across the indoor space.

4.2. Optimization Scenarios

To investigate the impact of transmission patterns, two distinct optimization scenarios were considered:

- Scenario P: The eight diffuse spots were uniformly arranged along the perimeter of a 0.5 m radius circle, creating a structured and predictable transmission pattern.
- Scenario Q: The eight diffuse spots were randomly distributed within the room, generating a more dynamic and unpredictable transmission environment.

Despite differing placements, the diffuse spot intensities remained non-uniform, with random distributions ensuring varied transmission characteristics. However, the total emitted power remained consistent at 2 W, standardizing energy output for comparative analysis.

Table 1 provides a comprehensive overview of the key simulation parameters utilized for both PSO and JAYA algorithms, highlighting essential system attributes that guided performance evaluation.

Table 1. Simulation parameters.

S/No	Parameter	Values
1	**PSO Algorithsm**	
	Nos of Iteration	100
	Nos of Particles	50
	Nos of Evaluations	5000
2	**Jaya Algorithsm**	
	Population size, N	100
	Dimension, D	4
	Room dimension	$4 \times 4 \times 3$
	Reflectivity of the wall	0.8
	Reflectivity of the ceiling	0.8
	Reflectivity of the wall	0.3
	Receivers location	(1.6, 2.1, 1), (4.8, 4.5, 1), (3.3, 0.7, 1), (0.4, 2.2, 1)
	Noise source location	(1.1.3), (1, 2, 3), (1, 3, 3), (1, 4, 3), (4, 1, 3), (4, 2, 3), (4, 3, 3), (4, 4, 3)
	Photodectetor (PIN)	0.5 A/W
	responsivity	
	Bit rate	100 Mbps
	Receive bandwidth	70 Mhz

To evaluate system performance, a controlled indoor simulation environment was designed, replicating real-world conditions within a 4 m × 4 m × 3 m room. Receivers were strategically positioned 1 m above the floor, ensuring varied signal propagation pathways.

$$F = \sum_{k=1}^{NR} (\omega_1 \times SNR_r - \omega_2 \times DS_k) \quad (9)$$

The fitness function used for optimization (Equation (9)) considered both delay spread (DS_k) and signal-to-noise ratio (SNR_r) at each of the NR receivers (Rxs). It is defined as follows:

$$Fitness = \omega_1 \times \sum DS_k + \omega_2 \times \sum \frac{1}{SNR_k} \qquad for\ k = 1\ to\ NR \quad (10)$$

where $\omega_1 = 1$ and $\omega_2 = 1 \times 109$ represent the weights assigned to each component of the fitness function. These weights balance the influence of delay spread and SNR_k on the overall optimization objective. The large value of ω_2 suggests a strong emphasis on maximizing SNR_r.

4.3. Impact of Delay Spread and Optimized DiS Configurations

Delay spread (DS_k) is a critical factor in optical wireless communication systems, as it directly influences the achievable bit rate and bandwidth (BW) at the receivers. Excessive DS_k can lead to intersymbol interference, reducing signal clarity and limiting transmission efficiency. To counteract these effects, DS_k is strategically incorporated into the fitness function, ensuring the optimization process prioritizes minimal signal dispersion while maximizing overall system performance.

4.4. Optimized DiS Placement and Intensity Distributions

Figure 3a,b illustrate two distinct scenarios for DiS placement and intensity allocation, highlighting their impact on receiver signal quality:

- Figure 3a—circular arrangement: Rxs 1 and 4 experience the highest susceptibility to noise due to their proximity to multiple noise sources. Conversely, Rxs 2 and 3 are less affected, since each one is near only one noise source, leading to improved signal reception and reduced interference.
- Figure 3b—scattered distribution: The intensity allocation reveals a significant power concentration in DiS 8, which exceeds the output of other DiSs. This is because DiS 8 is tasked with simultaneously serving two receivers (Rxs 1 and 3), with Rx 3 positioned farther away. To ensure reliable signal transmission at greater distances, DiS 8 must emit higher power, compensating for signal attenuation over the propagation path.

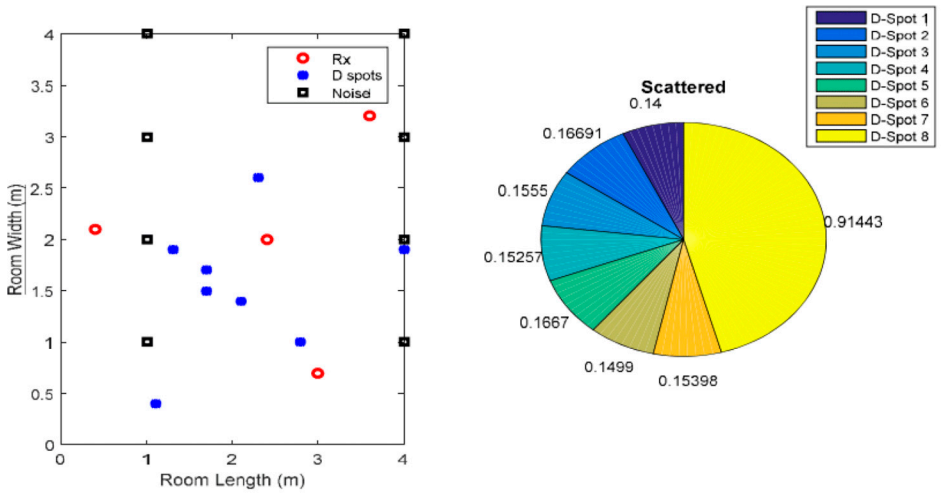

(**a**) (**b**)

Figure 3. (**a**) Scattered distribution of DiSs spot and (**b**) intensities of the diffused spots post-optimization (scattered distribution).

These findings underscore the importance of strategic DiS placement and intensity adjustments, reinforcing their role in optimizing SNR, delay spread minimization, and overall transmission efficiency. By adapting emission characteristics based on receiver location and environmental factors, optical wireless systems can achieve superior performance, ensuring stable and high-quality data delivery across diverse indoor settings.

The diffuse spots were placed at sufficient distances from the corners of the room in the range >0.4 and <3 in order to actualize the optimized locations of the diffuse spots.

4.5. Optimized Diffuse Spot Placement and Performance Analysis

Figure 4 presents results from the second scenario, demonstrating how optimized diffuse spot (DiS) placement enhances system performance. The strategic positioning of DiSs closer to their respective receivers (Rxs) ensures improved signal transmission:

- S2 and S3 align near Rx3, optimizing coverage.
- S1, S6, and S7 cluster around Rx2, reinforcing signal stability.
- S4 and S8 support Rx4, mitigating interference.
- S5 targets Rx1, optimizing transmission efficiency.

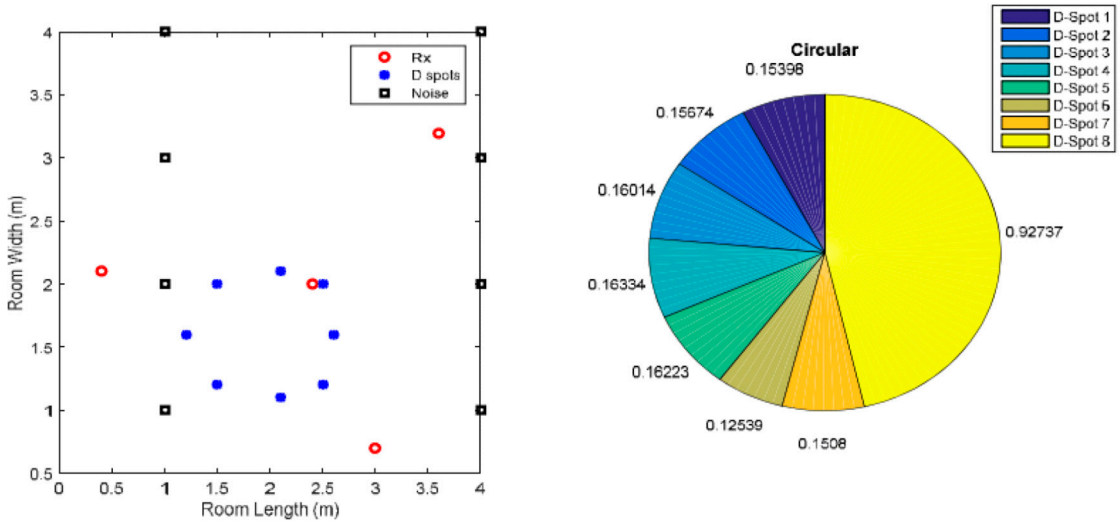

(**a**) (**b**)

Figure 4. Optimized parameter for the diffuse spot of the first scenario (i.e., circular) from the top. (**a**) Circular distribution of DiSs spot; (**b**) intensities of the diffused spots optimized circular.

Notably, Rx1 and Rx4 are positioned near noise sources, making them more vulnerable to interference.

4.6. Intensity Distribution and Signal Optimization

Figure 4b reveals that S8 exhibits a higher power level than other DiSs. This is because S8 serves Rx4 while simultaneously being close to Rx1, both of which are nearby noise sources. The increased intensity of S8 compensates for signal degradation, leading to higher SNR values at Rx1 and Rx4. This distribution ensures a more uniform SNR balance across all receivers, stabilizing communication performance.

4.7. Comparative Performance Analysis

Table 2 and Figure 5 provide a detailed comparison of key system metrics, evaluating average SNR, DS, standard deviation of SNR, and standard deviation of delay spread across different optimization scenarios:

- Scenario 1—Initial unoptimized configuration.
- Scenario 2—Optimized DiS placement for refined signal transmission.
- Scenario X—Centrally positioned DiSs with uniform power distribution.
- Scenario Y—JAYA-optimized DiS distribution for maximum efficiency.

Key observations from JAYA vs. PSO optimization:

- Optimized center placement (JAYA vs. PSO):
    - JAYA's center-based optimization yielded a 23.26% improvement in average SNR and a 28.87% improvement in SNR standard deviation over PSO.

- Average DS improved by 19.7%, indicating better temporal signal distribution compared to Scenario 1's unoptimized layout.
- JAYA also demonstrated faster convergence and better delay spread control, though Scenario 1 exhibited slightly better standard deviations for SNR and DS.

- Optimized locations and intensities (Scenario 2):
  - Refining both the placement and intensity of randomly distributed DiSs in Scenario 2 led to a 1.76% increase in average SNR and a 12% reduction in average DS relative to Scenario 1.
  - JAYA's optimization outperformed PSO in DS standard deviation, though reference [8] reported slightly superior DS standard deviation results.

Table 2. Comparison of the optimization scenarios using PSO.

Optimized Scenarios	Average Delay Spread (s)	STD of DS	Average SNR (dB)	STD of SNR
Scenario X [11]	1.0270×10^{-9}	0.8462×10^{-9}	17.9881	3.5656
Scenario Y [11]	0.9528×10^{-9}	0.5833×10^{-9}	19.4327	1.1508
Scenario 1	0.90296×10^{-9}	0.5095×10^{-9}	19.8667	1.0781
Scenario 2	0.85615×10^{-9}	0.4880×10^{-9}	22.7776	0.9974

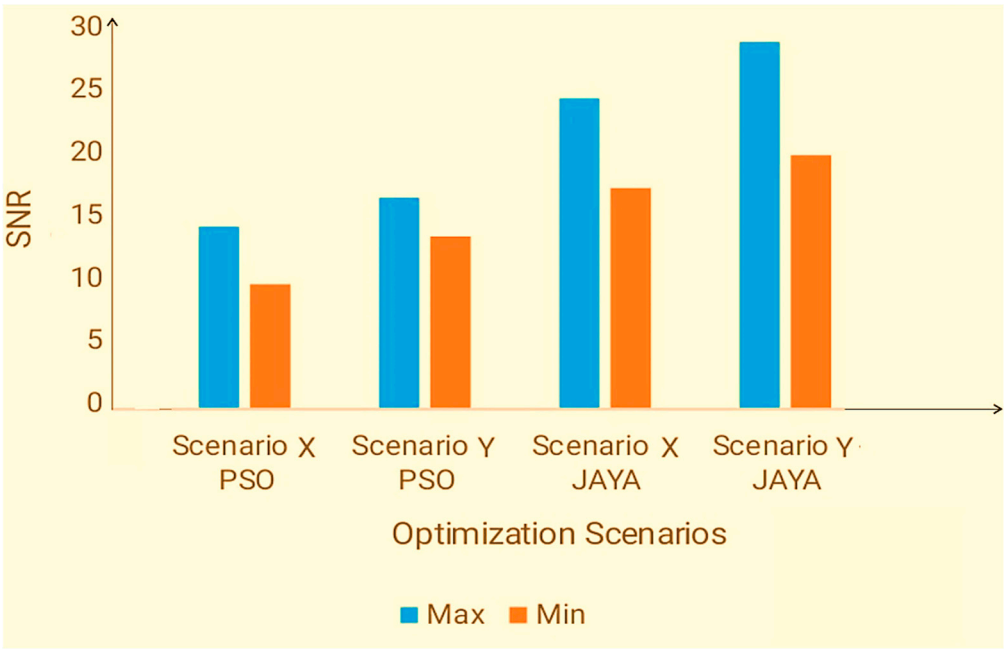

Figure 5. Minimum and maximum SNR obtained.

4.8. Impact of Variable Count on Optimization

Scenario 2 introduced 24 adjustable variables, exceeding Scenarios Y (2) and 1 (10), providing greater adaptability in DiS adjustments based on environmental factors. This higher degree of flexibility explains the observed improvements in SNR, DS, and SNR standard deviation.

Figure 4 visually highlights how optimized parameter tuning enhances DiS placement, enabling the system to intelligently adjust transmission characteristics for maximum efficiency and stable performance. Expanding optimization parameters allows greater precision, ensuring optimal wireless communication quality across dynamic indoor environments.

4.9. Analysis of SNR and Delay Spread Across Optimization Scenarios

A comparative evaluation of SNR and DS across multiple scenarios provides key insights into system performance improvements and trade-offs as presented in Table 3.

Table 3. Comparison of the optimization scenarios.

Optimized Scenarios	Average Delay Spread (s)	STD of DS	Average SNR (dB)	STD of SNR
Scenario 1	0.8284×10^{-9}	0.395×10^{-9}	24.6022	0.9422
Scenario 2	0.7306×10^{-9}	0.3595×10^{-9}	25.042	0.8990

4.9.1. Scenario 1 vs. Scenario 2: Performance Trade-Offs

Scenario 1 represents the initial setup, exhibiting solid SNR and delay spread values. However, Scenario 2, which incorporates optimized DiS locations and intensities, demonstrates measurable improvements:

- A 1.76% increase in average SNR;
- A 12% reduction in average DS.

Despite these gains, Scenario 2 introduces a higher standard deviation in SNR, reflecting a broader variation across receivers. Applying the Jaya algorithm, the delay spread standard deviation in Scenario 2 outperforms PSO, though it remains slightly worse than the reference [8].

4.9.2. Variable Count and System Adaptability

Scenario 2 benefits from an expanded optimization variable set (24) compared to Scenario Y (2) and Scenario 1 (10), giving it greater adaptability in refining the DiS configuration. This increased flexibility enables precise DiS positioning around the receivers (Figure 4), leading to significant improvements in the SNR and DS.

4.9.3. Evaluating SNR Stability (Figure 5-SNR Bar Chart)

Figure 5 visually contrasts the maximum and minimum SNR values across the four scenarios:

- Scenario Y (Jaya optimization) improves the minimum and average SNR, reducing the difference between max/min SNR, leading to a more stable SNR standard deviation (Table 2).
- Scenario 1 exhibits a higher max, min, and average SNR than Scenario A, but its standard deviation is higher due to the greater disparity between max/min SNR values.
- Scenario 2 shows broad improvements in average, min, and max SNR, yet displays a 2.8 dB gap between max/min SNR values. This difference suggests that while average SNR improves, the variation across receivers increases, impacting stability.

4.9.4. Eye Safety Considerations in Real-World Applications

In practical implementations, eye safety regulations must be prioritized when determining maximum transmit power. Factors such as DiS placement, number of transmitters, and Lambertian reflection properties all play crucial roles in ensuring compliance. While this study focuses on impulse response-based proof-of-concept optimization, real-world deployments must strictly adhere to safety standards, reinforcing operational integrity.

The analysis highlights the benefits and trade-offs of optimization algorithms, emphasizing the role of variable count, adaptability, and DiS placement in improving SNR and delay spread. By refining DiS positioning and intensity, optical wireless systems

can enhance communication stability while addressing safety constraints for real-world applications.

4.10. Focus on Signal-to-Noise Ratio Optimization

With the DS values successfully meeting the constraints for a maximum bit rate of 100 Mbps, the optimization emphasis now shifts toward SNR, as depicted in Figure 5.

By achieving acceptable DS levels, the system effectively minimizes intersymbol interference, ensuring stable high-speed data transmission. However, SNR remains a crucial determinant of communication reliability, as it directly impacts signal clarity, reception quality, and error rates across the transmission channel.

Figure 5 highlights how refined DiS placement and intensity adjustments influence SNR distribution, optimizing overall performance and signal stability. Higher SNR values across receivers translate to improved transmission fidelity, reinforcing the system's capacity to operate under dynamic indoor conditions.

This strategic focus on SNR enhancement ensures a robust optical wireless communication framework, capable of supporting efficient data transmission, minimizing noise interference, and providing superior overall connectivity.

5. Conclusions

This study explored the optimization of DiS placement and intensity in indoor visible light OWC systems, with the primary objective of SNR and minimizing DS. By analyzing various optimization scenarios, this research assessed how the number of optimization variables impacts SNR and DS performance across different user environments.

Key Findings and Impacts:

- Significant performance gains: the Jaya algorithm demonstrated its effectiveness by achieving up to a 29% improvement in SNR and a 23.3% reduction in delay spread, reinforcing its superiority in signal refinement.
- Enhanced stability: the optimization process contributed to better standard deviations in SNR (up to 5%) and delay spread (up to 9.9%), ensuring greater consistency in performance despite challenges such as ambient light interference and multipath dispersion.
- Hybridization and increased variable count: This study highlights the advantages of combining optimization algorithms while expanding the number of adjustable variables. This approach enhances the adaptability of diffuse spots, allowing them to dynamically adjust to environmental conditions, ultimately boosting overall system efficiency and communication reliability.

Final Implications:

These results affirm the importance of strategic optimization in optical wireless systems, demonstrating how adaptive placement and intensity control can significantly improve SNR stability, delay spread management, and signal transmission quality. Future research could further refine hybrid algorithm approaches to enhance real-time adaptability, ensuring robust high-speed communication in diverse indoor environments.

Author Contributions: Conceptualization, A.B.B.; methodology, A.B.B.; software, A.B.B.; validation, A.B.B.; formal analysis, A.B.B.; investigation, A.B.B.; resources, A.B.B.; data curation, A.B.B.; writing—A.B.B.; writing—review and editing, M.D., T.E.M., and A.D.M.; visualization, A.B.B.; supervision, M.D., S.Z., T.E.M., S.S.O., and A.U.U., project administration, A.B.B.; funding acquisition, S.S.O., A.D.M., and T.E.M. All authors have read and agreed to the published version of the manuscript.

Funding: This research received no external funding. The APC was co-funded by the NCC Professorial Chair Endowment, Federal University of Technology, Minna, Niger State; Department of Industrial Design, Modibbo Adama University, Yola, Adamawa State; and Department of Information Technology, Tshwane University of Technology, Pretoria, South Africa.

Data Availability Statement: The original contributions presented in this study are included in the article. Further inquiries can be directed to the corresponding author.

Conflicts of Interest: The authors declare no conflicts of interest. The funders had no role in the design of the study; in the collection, analyses, or interpretation of data; in the writing of the manuscript; or in the decision to publish the results.

References

1. Agiwal, M.; Roy, A.; Saxena, N. Next generation 5G wireless networks: A comprehensive survey. *IEEE Commun. Surv. Tutor.* **2016**, *18*, 1617–1655. [CrossRef]
2. Alsulami, O.; Hussein, A.T.; Alresheedi, M.T.; Elmirghani, J.M.H. Optical wireless communication systems: A survey. *arXiv* **2018**, arXiv:1812.11544. [CrossRef]
3. Arfaoui, M.A.; Soltani, M.D.; Tavakkolnia, I.; Ghrayeb, A. Measurements-based channel models for indoor LiFi systems. *IEEE Access* **2020**, *20*, 827–842. [CrossRef]
4. Chowdhury, M.Z.; Shahjalal, M.; Hasan, M.K.; Jang, Y.M. The Role of Optical Wireless Communication Technologies in 5G/6G and IoT Solutions: Prospects, Directions, and Challenges. *Appl. Sci.* **2019**, *9*, 4367. [CrossRef]
5. Javaid, F.; Wang, A.; Sana, M.U.; Husain, A.; Ashraf, I. Characteristic study of visible light communication and influence of coal dust particles in underground coal mines. *Electronics* **2021**, *10*, 883. [CrossRef]
6. Khalighi, M.A.; Ghassemlooy, Z.; Alouini, M.S.; Hranilovic, S.; Zvanovec, S. Optical wireless communications for emerging connectivity requirements. *IEEE Open J. Commun. Soc.* **2021**, *2*, 82–86. [CrossRef]
7. Kirrbach, R.; Faulwaßer, M.; Jakob, B.; Schneider, T.; Noack, A. Li-Fi for augmented reality glasses: A proof of concept. In Proceedings of the 2019 IEEE International Symposium on Mixed and Augmented Reality Adjunct (ISMAR-Adjunct), Beijing, China, 10–18 October 2019; pp. 263–268.
8. Lebaka, M. Optimization of spot pattern in indoor diffused optical wireless systems. *IEEE Photonics Technol. Lett.* **2006**. Available online: https://home.iitk.ac.in/ ynsingh/mtech/lmadhu.pdf (accessed on 9 August 2025).
9. Manousiadis, P.; Yoshida, K.; Turnbull, G.A.; Ifor, D.W.; Samuel, I.D.W. Organic semiconductors for visible light communications. *Phil. Trans. R. Soc. A.* **2020**, *378*, 20190186. [CrossRef] [PubMed]
10. Alves, L.N.; Khalighi, M. Optimization and design of a diffuse optical wireless sensor network. *Appl. Opt.* **2022**, *61*, 6599–6608. Available online: https://opg.optica.org/ao/abstract.cfm?uri=ao-61-22-6599 (accessed on 9 August 2025). [CrossRef] [PubMed]
11. Eltokhey, M.W.; Mahmoud, K.R.; Ghassemlooy, Z.; Obayya, S.S.A. Optimization of intensities and locations of diffuse spots in indoor optical wireless communications. *Opt. Switch. Netw.* **2019**, *33*, 177–183. [CrossRef]
12. Wong, D.W.K.; Chen, G.C.K. Optimization of spot pattern in indoor diffuse optical wireless local area networks. *Opt. Express* **2005**, *13*, 3000–3014. [CrossRef] [PubMed]
13. Wu, X.; Soltani, M.D.; Zhou, L.; Safari, M.; Haas, H. Hybrid LiFi and WiFi networks: A survey. *IEEE Trans. Wirel. Commun.* **2020**, *23*, 1398–1420. [CrossRef]
14. Chen, X.; Li, C.; Chen, L.; Wang, H.; Zang, Y.; Yao, W. Influence of different structure and specification parameters on the propagation characteristics of optical signals generated by GIL partial discharge. *Energies* **2020**, *13*, 3241. [CrossRef]
15. Zhou, H.; Chabory, A. An Extraction Method for the Multipath Characteristics of Simulated Tropospheric Propagation Channels. *IEEE Trans. Aerosp. Electron. Syst.* **2025**, *61*, 14401–14413. [CrossRef]